PRELIMINARY REGIONAL SEQUENCE STRATIGRAPHIC FRAMEWORK AND CHARACTERIZATION OF POTENTIAL FLUVIAL RESERVOIRS OF THE UPPER MESAVERDE GROUP, UINTA BASIN, UTAH

by Jennifer L. Aschoff

OPEN-FILE REPORT 569
UTAH GEOLOGICAL SURVEY
a division of
UTAH DEPARTMENT OF NATURAL RESOURCES
2010

PRELIMINARY REGIONAL SEQUENCE STRATIGRAPHIC FRAMEWORK AND CHARACTERIZATION OF POTENTIAL FLUVIAL RESERVOIRS OF THE UPPER MESAVERDE GROUP, UINTA BASIN, UTAH

by Jennifer L. Aschoff

Department of Geology and Geological Engineering
Colorado School of Mines
Golden, CO 80403

OPEN-FILE REPORT 569
UTAH GEOLOGICAL SURVEY
a division of
UTAH DEPARTMENT OF NATURAL RESOURCES
2010

STATE OF UTAH
Gary R. Herbert, Governor

DEPARTMENT OF NATURAL RESOURCES
Michael Styler, Executive Director

UTAH GEOLOGICAL SURVEY
Richard G. Allis, Director

PUBLICATIONS
contact
Natural Resources Map & Bookstore
1594 W. North Temple
Salt Lake City, UT 84116
telephone: 801-537-3320
toll-free: 1-888-UTAH MAP
Web site: mapstore.utah.gov
email: geostore@utah.gov

UTAH GEOLOGICAL SURVEY
contact
1594 W. North Temple, Suite 3110
Salt Lake City, UT 84116
telephone: 801-537-3300
Web site: geology.utah.gov

CONTENTS

FIGURES

TABLES

PLATES

PRELIMINARY REGIONAL SEQUENCE STRATIGRAPHIC FRAMEWORK AND CHARACTERIZATION OF POTENTIAL FLUVIAL RESERVOIRS OF THE UPPER MESAVERDE GROUP, UINTA BASIN, UTAH

EXECUTIVE SUMMARY

The Natural Buttes Gas Field, northeastern Utah, is one of the largest natural gas fields in the United States with more than 166 billion cubic feet of gas (BCFG) proved reserves. Natural gas production in the Natural Buttes area is primarily from tight-gas sands within Cretaceous and Tertiary strata, including much of the upper Mesaverde Group. Despite increased interest in the upper Mesaverde Group, pragmatic timelines and sound regional correlations for this interval in the Uinta basin are scant. Moreover, the regional sequence-stratigraphic framework and facies distribution is poorly understood. Carefully linking outcrop observations (i.e., detailed lithofacies, stacking patterns, flooding surfaces, regional unconformities, paleocurrents and detrital sandstone modes) to nearby subsurface data provides critical insight that can vastly improve regional correlations by and place productive facies within a regional context.

The goal of this pilot study was to construct a preliminary, outcrop-to-subsurface, sequence-stratigraphic correlation for the Price River and Farrer Formations from Price, UT to the Utah-Colorado state line. Deliverables for this study include: (1) a regional stratigraphic cross section; (2) 10 detailed stratigraphic profiles; (3) 2 interpreted outcrop photo mosaics with corresponding gamma-ray responses.

Unlike previous correlations that primarily use formation tops and net-to-gross patterns to correlate, this study used flooding surfaces, regional unconformities, detailed lithofacies, facies stacking patterns/architecture, sandstone composition and paleocurrents in outcrop to improve the regional, subsurface correlation. Two flooding surfaces were particularly useful for constructing the regional correlation, and making the critical link from the outcrop to the subsurface. Flooding surfaces were identified in outcrop by the presence of tidal- and marine-influenced units that suggest incursion of brackish to open-marine conditions into predominantly fluvial successions; they can be identified by their higher gamma-ray (GR) response compared to fluvial sandstones, and slightly lower GR response compared to floodplain sandstones with a characteristic “spiky” character and higher organic content. In addition, an up-section increase in detrital feldspar in sandstones of the upper Farrer Formation correspond to an up-section increase in the GR response of sandstones.

Outcrop analysis and correlation of outcrop and subsurface data suggest that subtle flooding surfaces and stratigraphic stacking patterns are the most useful for correlating long distances (> 50 km) in the Price River and Farrer Formations. Changes in fluvial stacking pattern, from clustered to isolated channel bodies, allow us to identify stratigraphic zones that may contain flooding surfaces. Careful examination of the GR and conductivity within these suspect zones helps to identify key flooding surfaces. Locally, unconformities are useful for correlation purposes. However, unconformities become more numerous and clustered near the northern extent of the San Rafael Swell; these unconformities appear to become conformable with distance away from the San Rafael Swell and may locally act as stratigraphic traps. It is possible that these unconformities form part of a large-scale growth-strata package on the margins of the San Rafael Swell. However, more detailed stratigraphic analysis is needed to fully understand the extent, character and genesis of these unconformities.

A distinct partitioning of depositional facies was recognized within the Price River and Farrer Formations. Stratigraphically, the lower part of this interval is a low net-to-gross sandstone succession with more isolated channel bodies, fewer crevasse splay deposits and less developed paleosols (thinner units with scare root traces and peds). Two important flooding surfaces are found within this lower stratigraphic interval. By contrast, the upper part of the Price River-Farrer succession is a higher net-to-gross sandstone interval with thicker and more amalgamated channel bodies, more crevasse splay deposits and better developed paleosols (thicker units with large, fully preserved root traces). Geographically, sandstone-rich intervals are more abundant on the distal flanks (>20 km) of the San Rafael Swell. Paleocurrents are highly variable, but are generally north- to northeast-directed currents that become more northerly in the vicinity of the San Rafael Swell.

Preliminary results from this study suggest that the San Rafael Swell deflected fluvial systems northward, and may have formed semi-regional unconformities along its crest and controlled accommodation patterns that influenced fluvial architecture and sand distribution.

INTRODUCTION

Project Scope and Objectives

The Natural Buttes Gas Field, northeastern Utah, is one of the largest gas fields in the United States with more than 166 BCFG proved reserves. Natural Buttes, and the surrounding region, is a key area of interest for many Rocky Mountain based energy companies, and promises to continue this trend with the opening of the new Chapeta Gas Processing Plant. Production in the Natural Buttes area is primarily from Cretaceous and Tertiary strata, including much of the upper Mesaverde Group.

Despite increased interest in the upper Mesaverde Group, pragmatic timelines for sound regional correlations are scant, and the regional sequence-stratigraphic framework and detailed facies distribution are poorly constrained. The purpose of this study was to fill the gaps in our knowledge concerning the sequence-stratigraphic framework and facies distribution within the upper Mesaverde Group. Unlike previous correlations that primarily use formation tops to correlate, this study used flooding surfaces, regional unconformities, detailed lithofacies, facies stacking patterns/architecture, sandstone composition and paleocurrents derived from outcrop description to improve the regional, subsurface correlation.

The two main goals of this research were to: (1) improve the regional sequence-stratigraphic framework of the upper Mesaverde Group (Price River and Farrer Formations), and (2) describe and interpret potential sandstone reservoirs within the Price River and Farrer Formations from Price UT to the UT-CO state line. To achieve these goals, a detailed subsurface-to-outcrop, stratigraphic cross section and two photo mosaics were constructed to show the types and distribution of potential reservoir facies in a regional framework. The database for this project consisted of 10 new, detailed stratigraphic profiles, 4 published stratigraphic profiles, 2 new, outcrop-based GR curves and 146 public well-logs. The stratigraphic cross section consisted of 10 new and 4 published stratigraphic profiles, two of which were complemented by outcrop GR curves, and about 20 published well-logs. Stratigraphic profiles and nearby well-logs were projected onto a roughly east-west cross-section line.

Objectives

To achieve the main goals of the study, three specific objectives were completed:

- Construct an integrated (for example, subsurface-to-outcrop) sequence-stratigraphic correlation of the Price River and Farrer Formations of the upper Mesaverde Group to establish pragmatic timelines for correlating the upper Mesaverde Group;
- Measure the outcrop gamma-ray response of key facies constituting the Price River and Farrer Formations in order to predict facies types, reservoir properties and key producing units in subsurface data;
- Describe the internal character, dimensions, geometry and distribution of fluvial and tidal-fluvial reservoirs within the Price River and Farrer Formations.

Study Area and Stratigraphic Focus

The outcrop component of this study focused on excellent exposures of the Price River and Farrer Formations of the upper Mesaverde Group that are present along the Book Cliffs (Figures 1 and 2). Exposures of the Price River and Farrer Formations are nearly continuous from Price to the UT-CO state line and generally trend East-West, except East of Sagers Canyon where they adopt a more northerly trend. The Book Cliffs provide two important dimensions for stratigraphic analysis, while integration with well-log data provides the third dimension. New stratigraphic profiles were measured at Willow Creek, Nine Mile Canyon, Horse Canyon, Turtle Canyon, Green River, Floy Canyon, Thompson Canyon, Cottonwood Canyon, Hays Canyon and San Arroyo Canyon (Figure 3).

Acknowledgements

This 7-month pilot study was partially funded by the Utah Geological Survey, whom I gratefully acknowledge. I thank Parker Valora and Sarah Edwards, MS Candidates at Colorado School of Mines, who helped build the GeoPlus PETRA project and draft stratigraphic profiles for this project. Given the short duration of the project, it would not have been possible to complete the deliverables without their help. Addi-

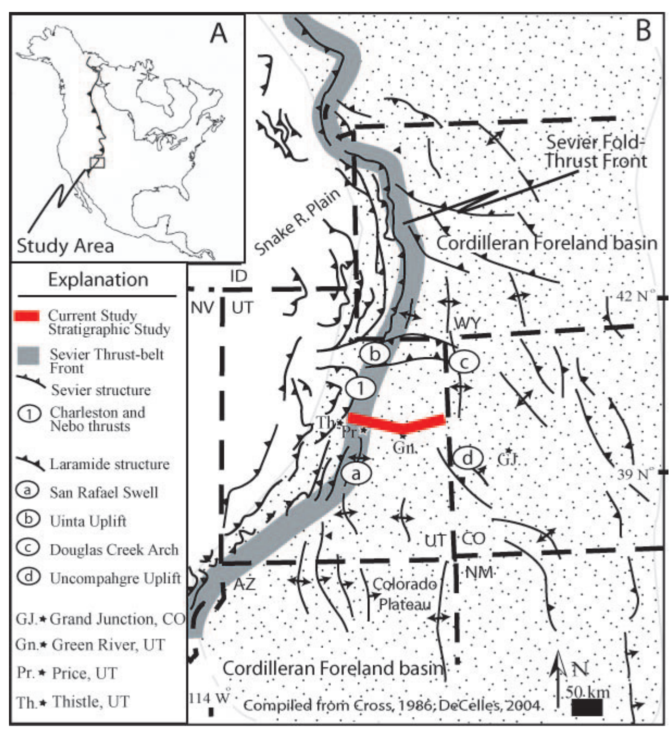

Figure 1. *Location and geologic context of the study area.*

tionally, I wish to thank Kyle Graff and Jeffrey Thompson for their help collecting field data. Komon Pinyo also measured two of the stratigraphic sections used in this study (Willow Creek and Turtle Canyon).

Stages/ Substages		Lithostratigraphic Units		Age (Ma)
		Price, UT	Green River, UT	
PALEOCENE	PALEOGENE	North Horn Fm.	Conglomerate at Dark Canyon	60.0
				65.0
UPPER CRETACEOUS	MAASTR.	Price River Fm.	Tuscher Fm.	
	CAMPANIAN		Farrer Fm.	
		Bluecastle T.	Bluecastle T.	75.0
		Middle and Lower Castlegate S.s	Neslen Fm., Sego S.s., Buck T., Castlegate S.s.	

Figure 2. *Stratigraphic correlation chart showing the stratigraphic study interval and approximate correlation to strata in adjacent basins. Ages are from Cobban and others 2006.*

GEOLOGIC CONTEXT

Tectonics and Basin Development

The Farrer and Price River Formations constitute part of the predominantly non-marine fill of the Cretaceous Cordilleran Foreland Basin. This foreland basin developed from the Jurassic through the Cretaceous as a result of flexure adjacent to the thickened crust of the Sevier fold-thrust belt (DeCelles, 2004). Deformation in the fold-thrust belt, and later in basement-cored structures, is attributed to the transfer of stress from the subduction zone at the western margin of North America, where oceanic lithosphere of the Farallon Plate was subducted below continental lithosphere of the North American Plate. During the development of the basin, sediment was generally transported from the thrust-belt in the west to the east, into the Western Interior Seaway. Thrust-belt proximal and younger foreland basin strata tend to be more non-marine, whereas more distal foreland basin strata tend to be more marine-influenced due to periodic incursions of the Western Interior Seaway.

During the late stages of foreland basin development, from the latest Cretaceous to Paleogene, basement-cored (i.e., "Laramide") structures locally punctuated the subsiding foreland basin (Dickinson and Snyder, 1978). These Laramide structures locally, and perhaps region-

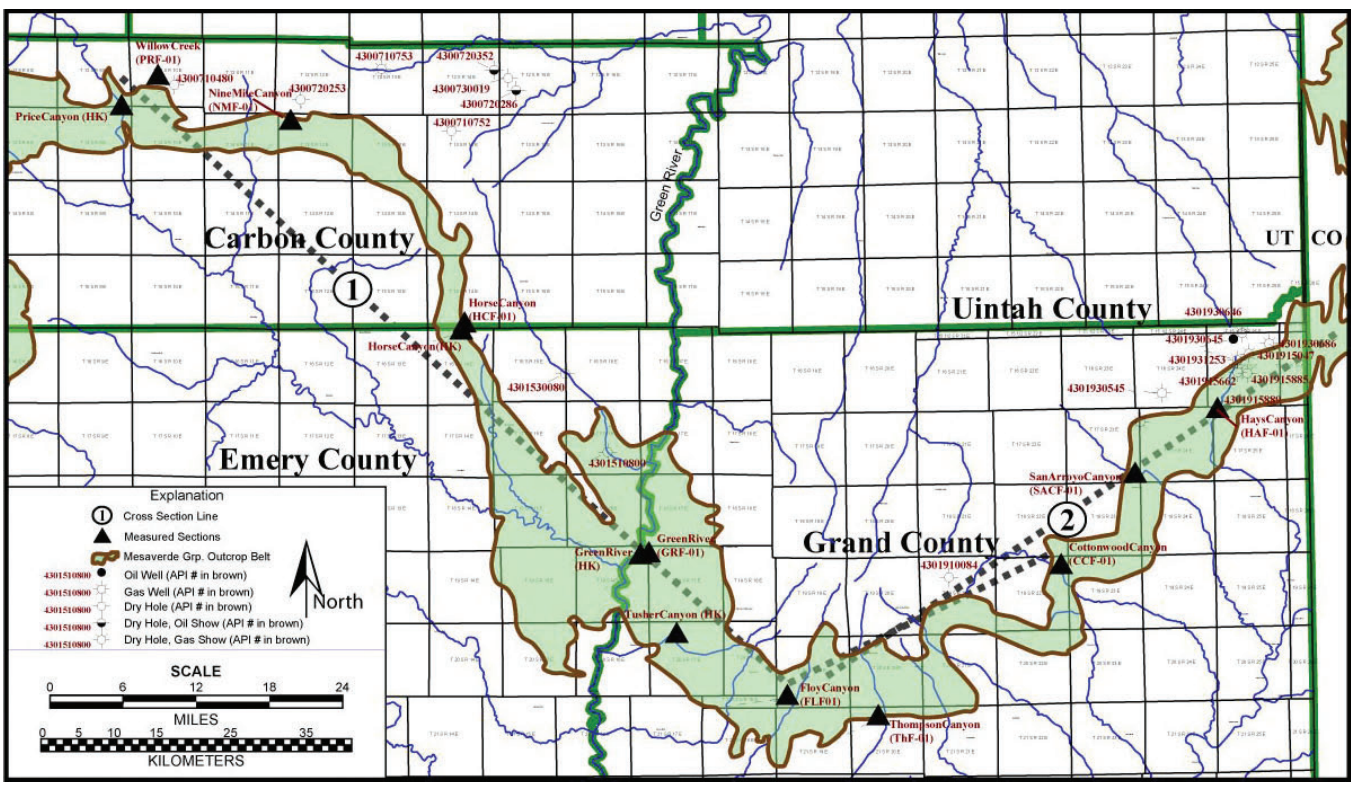

Figure 3. *Map of the study area showing the location of wells (circles) and stratigraphic profiles (triangles) compiled in the database, outcrops of Mesaverde Group (light green) and basic geography of the southern Uinta basin. Datum is NAD 1927, Zone 12. Land grid is in townships. Click here to view enlarged figure. Geology shapefiles are from Hintze and others (2000).*

ally, altered accommodation patterns and caused deflection of sediment dispersal systems. During phases where Laramide-style uplift exceeded sedimentation rate these structures may have developed relief and provided a small amount of sediment to adjacent depositional systems. Basement-cored structures present in Central Utah include the San Rafael Swell and Uinta Uplift. The San Rafael Swell, one of several enigmatic uplifts on the Colorado Plateau, has been interpreted as a Laramide structure. Although basement is not exposed in the San Rafael Swell, seismic and gravity data suggest that it is cored by basement (Bump and Davis, 2003). In particular, the San Rafael Swell has been shown to have been active since 77 Ma (Aschoff, 2008). Although this structure was probably not a significant source of sediment, it may have deflected fluvial systems of the Price River and Farrer Formation. Moreover, semi-regional unconformities (~10-50 km) may have developed along the crest of the San Rafael Swell. The Uinta Uplift is thought to be much younger than the San Rafael Swell and was probably not significantly affecting sediment dispersal patterns; however, more work is needed to determine if, and how the Uinta Uplift may have influenced sedimentation patterns in the Maastrichtian to Paleogene interval.

Sediment for the Farrer and Price River Formations is thought to have been largely derived from the Sevier fold-thrust belt. However, Laramide structures such as the San Rafael Swell may have had a considerable influence on sediment dispersal patterns, fluvial architecture and faceis stacking patterns, and the development of unconformities. And, the influence of the "Proto-Uinta Uplift" on Maastrichtian deposition is largely unknown.

Stratigraphy

Speiker (1946) and Fisher and others (1960) were among the first workers to define the stratigraphy in the Book Cliffs area, and recognize the thick succession of strata constituting the Price River and Farrer Formations. Later, Fouch and others (1982) provided chronostratigraphic evidence that the Price River and Farrer Formations were age-equivalent. However, the precise correlation of the Price River Formation to the Farrer Formation, and the evolution of the depositional systems responsible for them have been somewhat contentious because their paleocurrents and sandstone compositions are quite different (Lawton, 1983; Lawton, 1986; Fouch and others, 1994; Olsen and others, 1995; Guiseppe and Heller, 1998). One of the key questions at the center of this debate is the role that the San Rafael Swell played in deflecting and/or segmenting sediment dispersal systems. Recent regional sequence-stratigraphic studies (Hettinger and Kirschbaum, 2002) support earlier workers (Fouch and others, 1982; Lawton, 1983) who correlate the Price River and Farrer Formations across the San Rafael Swell (Figure 1). However, some workers contend that uplift along the San Rafael Swell caused northward deflection of fluvial systems and that the depositional systems for the Price River and Farrer Formations are time-correlative but distinct fluvial systems. Resolving questions about the correlation and depositional history of these units has implications for predicting the distribution of potential reservoirs, seals and traps. Previous studies have addressed the stratigraphy of the Price River and Farrer Formations, but many of these studies were local, or did not provide a high level of detail. The present study provides another level of detail within part of this succession with a more extensive sequence-stratigraphic correlation that integrates a wide array of subsurface and detailed outcrop data.

METHODS AND DATASET

The present research integrates outcrop with subsurface data to construct a regional correlation of part of the upper Mesaverde Group in northeastern Utah and characterize potential reservoirs within this interval. Outcrop data consisted of 10 detailed (20 cm scale), 200-400 m long stratigraphic profiles measured at a 10-mile (km) spacing wherever possible and two photo mosaics that delineates the geometries, dimensions and internal character of sandstone bodies within the Price River and Farrer Formations. Stratigraphic profiles made special note of depositional facies, facies stacking patterns, key sequence-stratigraphic surfaces, evidence of marine/tidal influence, visually estimated detrital sandstone composition and paleocurrent direction. The outcrop data were supplemented with four published stratigraphic profiles that were compiled by Hettinger and Kirschbaum (2002).

Outcrop gamma-ray responses (total counts per second, cps) of the facies were measured for 2 of 10 new stratigraphic profiles. The GR responses were measured with a GR Spectrometer at 1-3 m increments wherever possible and keyed to detailed descriptions and observations in each stratigraphic profile. Spectrometer data were recorded by the internal data logger, uploaded to Microsoft Excel™ and imported to GeoPlusPETRA™ where they were converted to LAS files and added to the PETRA project. GR responses were also plotted on photomosaics to delineate the gamma-ray responses of sandstone bodies. These outcrop data were closely linked to nearby subsurface data using the gamma-ray responses from the outcrop.

Subsurface data used in the cross-section consisted of 20 public well-logs that were downloaded from the Utah Division of Oil, Gas, and, Mining (DOGM) website. Wells with GR and spontaneous potential (SP) curves that were located < 5 miles from the Book Cliffs outcrop belt were preferentially selected for the database. Tops data were compiled from the DOGM website and U.S. Geological Survey (USGS) National Oil and Gas Assessment (NOGA) websites and systematically corrected. New formation tops and flooding surface tops supplemented these data.

The database, consisting of 10 new stratigraphic profiles, 4 published stratigraphic columns, 2 outcrop GR curves, 146 public well-logs (including the 20 used in the cross-section) and tops from the USGS and DOGM, was built using GeoPlus PETRATM . The datum for the project is North American Datum 1927, Zone 12. The stratigraphic profiles and public well-logs were depth-registered and correlated to subsurface data by direct comparison from the outcrop, northward into the subsurface. The two stratigraphic cross sections were constructed using the 10 new stratigraphic profiles, 4 published stratigraphic profiles and 20 publicly available well logs. Future work (planned for 2010) will incorporate the additional public well-logs to provide a more 3-dimensional stratigraphic framework and isopach maps of the Price River and Farrer Formations.

LITHOFACIES AND DEPOSITIONAL ENVIRONMENTS

Lithofacies were distinguished based on internal characteristics such as color, grain-size, bedding, sedimentary structures, grading and continuity of beds. These lithofacies were then grouped into non-genetic facies assemblages based on similar characteristics. This study defines 3 lithofacies assemblages and 13 distinct lithofacies within the Farrer and Price River successions. In general, it is difficult to distinguish all 13 facies in well-logs, however the 3 lithofacies assemblages, and in some cases individual facies, have distinct GR signatures that allow them to be linked directly to nearby subsurface data. Each of the 3 main lithofacies assemblages also have distinct reservoir characteristics, including differing degrees of internal heterogeneity and external dimensions. Although additional work is needed to fully characterize potential reservoirs, this study interprets each assemblage and qualitatively assesses two main potential reservoir types.

Assemblage A: Mudstone Facies

Description

Lithofacies Assemblage A consists of carbonaceous shale, massive mudstone and siltstone that locally contain root traces and peds (Table 1). Facies A1 forms continuous beds (10-50 cm thick) of structureless, carbonaceous shale and mudstone; it tends to be adjacent to sandstone facies C1 and C5. Facies A2 consists of medium-bedded (10-25 cm thick) laterally discontinuous beds of structureless siltstone with root traces. Facies A2 laterally grades into Facies A3, which is a distinctive, olive green colored, medium bedded (10-25 cm thick) structureless mudstone and siltstone (Figure 4). Facies A3 forms semi-continuous (100-1000 m) beds and locally contains pervasive carbonaceous root traces and blocky peds. Facies within this asseblage were not typically fractured in the study area (i.e., Book Cliffs area).

Interpretation

The mudstone facies constituting Lithofacies Assemblage A are generally interpreted as a series of floodplain deposits (Table 1). Facies A1, A2 and A3 are all fine-grained (i.e., clay and silt) and are not typically interbedded with sandstone, although some facies laterally grade into sandstone-rich intervals. Facies A1, carbonaceous shale, is interpreted as organic-rich suspension deposits due to the fine grain-size and horizontal lamination (Figure 4). Because these facies are commonly cut by adjacent channel-sandstones and are lateral to some channel facies, they may have been formed in a floodplain environment, possibly part of an oxbow lake or abandoned channel on the periphery of the main channel.

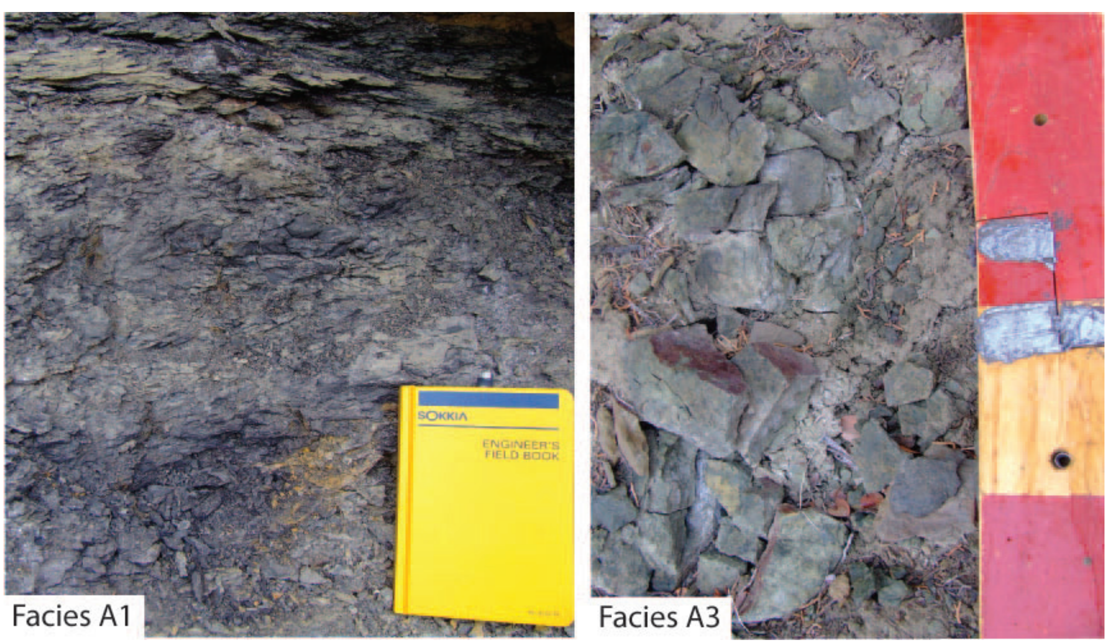

Figure 4. *Examples of facies constituting the mudstone facies assemblage.*

Table 1. Lithofacies descriptions and interpretations for Lithofacies Assemblage A-Mudstone Facies.

Assemblage A- Mudstone Facies			
Facies	Description	Interpretation	Environment
1	Medium- to thick-bedded (10-50 cm), black and gray, continuous beds of carbonaceous shale and structureless carbonaceous mudstone.	Suspension deposition	Floodplain (Oxbow Lake Fill (?), abandoned channel)
2	Medium-bedded (10-25 cm), brown and tan, discontinuous beds of structureless siltstone. Typically adjacent to, and interfinger with facies A3.	Traction transport followed by suspension deposition and pedogenesis	Floodplain
3	Medium-bedded (10-25 cm), green and brown, semi-continuous beds of mottled, structureless mudstone and siltstone with root traces. Root traces and carbonaceous rootlets are locally pervasive, with rootlets up to 20 cm long.	Suspension deposition followed by pedogenesis	Floodplain

Facies A2 typically contains a higher proportion of silt-sized sediment suggesting that there may have been phases of traction transport, or higher-energy conditions capable of entraining predominantly silt-sized material, that alternated with suspension deposition. Locally the facies contains root traces and blocky peds, which suggest a phase where the sediments were bioturbated and colonized by plants. The cyclic influx of silt-sized material followed by suspension deposition and later bioturbation by roots suggests that this facies was formed in the floodplain environment.

Facies A3 contains the highest density of root-traces and has a well-mixed, mottled fabric that suggests that this facies was developed on the floodplain. However, due to the higher proportion of root traces and bioturbation suggests that these sediments were exposed to pedogenesis for longer periods of time, and may have developed further away from the main fluvial channel that would normally provide sediment to the floodplain.

Reservoir Characteristics

Assemblage A can be identified on the GR log due its "spiky" character, and GR signatures that range from about 37 cps to 58 cps (Figure 5A, 5B). The facies constituting Facies Assemblage A are generally very well-mixed, fine-grained (clay- and silt-sized) and would not typically be considered reservoir quality. However, in some cases, the facies within Assemblage A (for example, Facies A3) may be prone to fracturing because of its heterogeneous internal character and semi-continuous (500-1000 m) geometry. Fracturing these facies would likely improve their performance.

Assemblage B: Heterolithic Facies

Description

Lithofacies Assemblage B is a complex suite of heterolithic facies; each contains a mixture of interbedded sandstone and/or mudstone, shale (Table 2). Facies B1 is a very thinly bedded (1-3 cm thick), current-ripple cross-laminated and horizontally laminated, very fine-grained sandstone with numerous carbonaceous shale drapes (< 1-2 cm) (Figure 6). Facies B2 forms lenticular beds (10-25 cm thick) with inclined (~5 degrees) sets of current-ripple cross-laminated and trough cross-stratified, fine- to very fine-grained sandstone with numerous carbonaceous mud drapes. Facies B3 forms sharp-based, lenticular beds (25-100 cm thick) of trough cross-stratified, fine-grained sandstone with superimposed current-ripple cross-laminated very fine-grained sandstone; subordinate carbonaceous mud drapes are present on cross-bed foresets. Locally, this facies contains mudstone rip-up clasts at the base of sandstone bodies and subordinate sigmoidal cross-bedding (Figure 6). Facies B4 is a very thin-bedded (1-3 cm thick) current-ripple cross-laminated, fine-grained sandstone with subordinate double mud-drapes and bi-directional ripple foresets; locally this facies contains 5-10 cm thick intervals of flaser-bedded, very fine- to fine-grained sandstone.

Interpretation

Facies constituting Facies Assemblage B record deposition within a wide range of environments including meandering fluvial, floodplain, tidally influenced fluvial, and estuarine environments. Ripple cross-laminated very fine-grained sandstone overlain by horizontally laminated fine-grained sandstone of Facies B1 records traction transport in the lower part of the lower flow regime followed by suspension deposition; this is consistent with deposition within a floodplain environment. Facies B2 was deposited within a meandering fluvial system that may have experienced seasonal variation in discharge. The sharp, erosive basal contacts and lenticular sandstone geometry of Facies B2 suggests deposition within a channel (Figure 6). Trough cross-bedded sandstone located near the toes of the inclined beds record traction transport in the upper part of the lower flow regime and grade into ripple cross-laminated sandstone near the upper part of the inclined bed recording traction transport in the lower part of the lower flow regime. Additionally, a distinct cyclicity consisting of higher-flow (trough cross-beds) to lower-flow (ripple cross-laminations) to suspension (mud drapes) conditions suggests seasonal (?) fluctuation in flow conditions (i.e., discharge). The presence of low-angle accretion sets with paleocurrent indicators that are oblique to the dip-direction of the inclined sets is consistent with deposition within a point bar, and ryth-

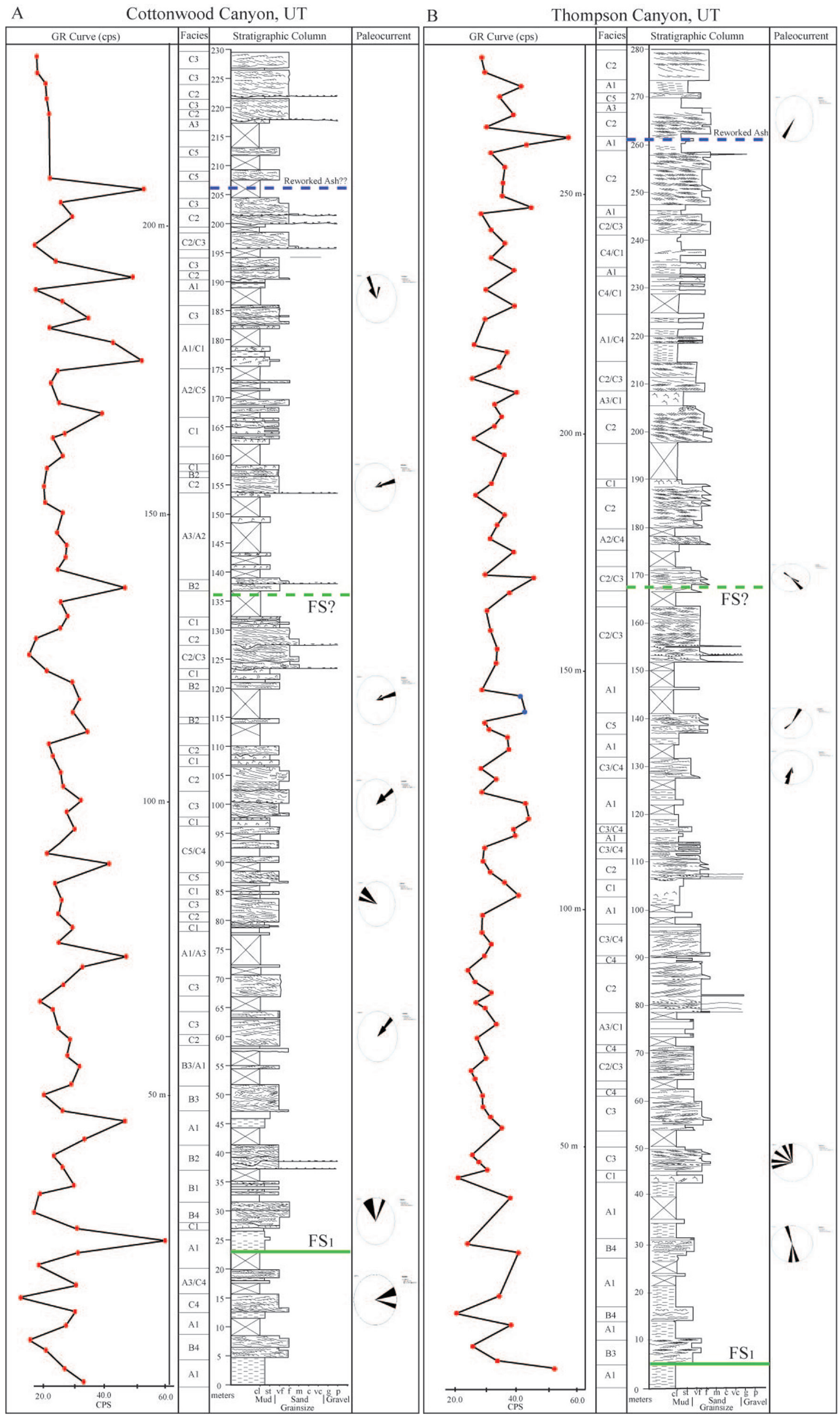

Figure 5. *Stratigraphic columns from A. Thompshon Canyon and B. Cottonwood Canyon showing the stratigraphic distribution of facies and GR response for those facies. Click here to view enlarged figure.*

Table 2. *Lithofacies descriptions and interpretations for Lithofacies Assemblage B-Heterolithic Facies.*

Assemblage B- Heterolithic Facies

Facies	Description	Interpretation	Environment
1	Very thin-bedded (1-3 cm), gray and tan, semi-continuous, ripple cross-laminated and horizontal-laminated, very fine-grained sandstone with numerous carbonaceous drapes. Forms paper-like partings.	Traction transport followed by suspension deposition	Floodplain
2	Medium-bedded (10-25 cm), gray to tan, lenticular beds of ripple and trough cross-stratified, fine- to very fine-grained sandstone with broad, low-angle inclined beds (lateral accretion sets) and numerous carbonaceous drapes.	Traction transport in the upper part of the lower flow regime with bidirectional flow or seasonal discharge	Meandering Fluvial Channel (with seasonal variation in discharge)
3	Thick-bedded (25-100 cm), gray and tan, sharp-based, lenticular beds of large-scale trough cross-stratified fine-grained sandstone with superimposed ripple cross-lamination, numerous carbonaceous drapes on cross-bed foresets and subordinate sigmoidal cross-bedding. Locally contains mudstone rip-up clasts.	Cyclic traction transport from the upper part of the lower flow regime to the lower part of the lower flow regime with bidirectional flow within a channel	Tidally Influenced Meandering Fluvial Channel
4	Very thin-bedded (1-3 cm), gray to tan, semi-continuous, ripple cross-laminated (bidirectional and unidirectional) fine-grained sandstone with subordinate double mud-drapes and 5-10 cm thick intervals of flaser-bedded, very fine- to fine-grained sandstone. Locally forms paper-like partings.	Cyclic traction transport from the lower part of the lower flow regime to suspension with bidirectional flow	Inner Estuary

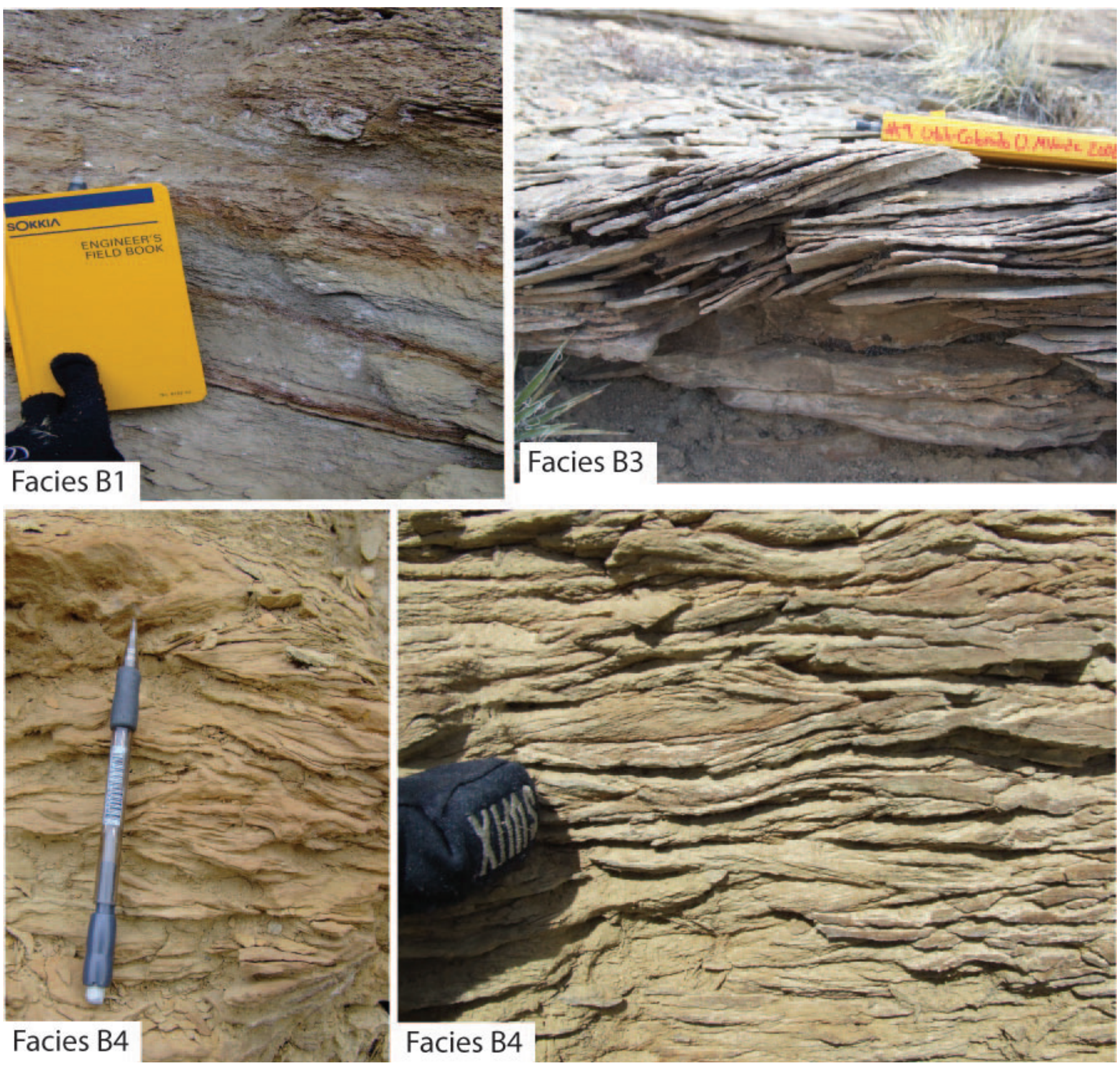

Figure 6. *Examples of facies constituting the heterolithic facies assemblage.*

mic cyclicity of sedimentary structures in the point bar suggests cyclicity, or seasonality, in the discharge of the fluvial system.

Facies B3 and B4 are interpreted as tidally influenced fluvial channels and inner estuarine deposits, respectively. The sharp, erosive basal contacts and lenticular sandstone geometry of Facies B3 suggests deposition within a channel, whereas the bi-directional flow indicators, numerous mud drapes, mudstone rip-up clasts and subordinate sigmoidal cross-bedding suggests tidal influence. Facies B4 has more apparent evidence of tidal influence due to the presence of double mud-drapes on bi-directional ripple cross-laminated sets, flaser bedding and numerous carbonaceous mud drapes and mud rip-up clasts on cross-beds. I interpret Facies B4 as deposits of an inner estuarine environment because there is an overall abundance of tidal indicators (i.e., double mud drapes, bi-directional current-ripple cross-lamination, flaser and lenticular bedding) the facies is typically muddier than facies B3.

Reservoir Characteristics

Facies constituting the heterolithic facies assemblage (Assemblage B) are generally sandy but contain numerous interbeds, lenses, and/or thin drapes of carbonaceous mudstone and shale. Although porosities may locally be higher-than-average, fluid flow and formation pressures are likely to be quite complex due to a wide range of heterogeneities; these include: (1) numerous small (2-10 m wide) channels, (2) large (10-1000 m wide) channels, (3) inclined beds, or lateral accretion sets, within the channels, (4) several types of cross-beds (trough and sigmoidal cross-beds and ripple cross-lamination) within the channels and/or superimposed on inclined beds, (5) abundant mudstone and shale interbeds (1-10 cm thick), and (6) zones with numerous, thin (<1 cm) carbonaceous mud drapes.

Sandstone bodies in this assemblage (Assemblage B) are generally single, isolated channels that generally range from 1-3 m thick and 10-200 m width. Although they are not typically amalgamated with other channels, they contain numerous other internal complexities related to accretion sets, bedding and mudstone drapes. These more heterolithc, heterogeneous sandstones are more abundant in the lower parts of the Farrer and Price River Formations. The sand-body dimensions provided in this study are approximate; much more work is needed to quantify the dimensions of the sandstone bodies. Comparatively, Facies B2 (meandering fluvial channels) will likely have the least number of internal heterogeneities, and relatively simple external geometry of all the facies in Assemblage B.

In well-logs, the heterolithic, sandstone-rich facies of Assemblage B are difficult to distinguish from “pure”, sandstone-dominated facies (Assemblage C), however the heterolithic facies tend to have a slightly higher GR signature (~25-35 cps) than the sandstones of Assemblage C (Figure 5A, 5B). A good example of the slightly higher GR signature of sandstones of Assemblage B is show in Figure 5A (Cottonwood Canyon Section) between 5m and 30m. However, GR measurements for Assemblage B are scant in the Thompson Canyon Section (Figure 5B) because these facies are not very abundant; in fact, two of three GR datapoints for Assemblage B facies in the Thompson Canyon section show a slightly lower GR response.

Assemblage C: Sandstone Facies

Description

Lithofacies Assemblage C consists of six fine- to medium-grained sandstone facies with a wide range of dimensions and sedimentary structures (Table 3). Facies C1 forms sharp-based, lenticular beds (10-25 cm thick) of structureless, fine-grained sandstone with root traces and relict ripple cross-laminations locally; this facies contains very little to no organic material intermixed with the sandstone. Facies C2 is a distinctive cliff-forming unit consisting of a sharp-based, thick-bedded (25-100 cm thick), broadly lenticular very fine- to fine grained sandstone with trough and planar-tabular cross-stratification (Figure 7). This facies tends to occur as a thick (1-6 m) succession of amalgamated lenticular units, and is relatively continuous (100-1000 m). Facies C3 is another cliff-forming facies that tends to be thinner and less extensive than C2 facies; C3 facies consists of 10-100 cm thick beds of laterally discontinuous, sharp-based trough cross-stratified and ripple cross-laminated, fine- to very fine-grained sandstone with subordinate low-angle, inclined bed-sets that have paleocurrents oblique to them (lateral accretion sets); carbonaceous shale locally defines the tops of the lateral accretion sets. Facies C4 is a very thin-bedded (1-3 cm thick) ripple cross-laminated, fine- to very-fine grained sandstone. Facies C5 forms semi-continuous (10-100 m), 10-25 cm thick beds of climbing-ripple cross-laminated, fine- to very-fine grained sandstone with subordinate trough cross-bedding. Facies C6 forms sharp-based, 10-25 cm thick, lenticular beds of planar-tabular and wedge-planar cross-bedded, fine- to medium-grained sandstone.

Interpretation

Lithofacies Assemblage C records deposition within a meandering fluvial environment. The sharp-based, lenticular to broadly lenticular sandstone beds with angle-of-repose cross-stratification and basal scouring suggests deposition of Facies C1, C2, C3, C5 and C6 by traction transport within channels. The low-angle bed-sets, superimposed with lower flow regime sedimentary structures (i.e., ripple cross-lamination, trough cross-bedding and planar-tabular cross bedding) are oblique to the dip-direction of the low-angle bed sets, of these sandstone bodies suggests deposition on laterally accreting point bars. Some facies (C1, C4) tend to be thinner bedded, have more bioturbation/root traces and have slightly lower energy sedimentary structures such as ripple cross-lamination; these

Table 3. *Lithofacies descriptions and interpretations for Lithofacies Assemblage C-Sandstone Facies.*

Assemblage C- Sandstone Facies			
Facies	Description	Interpretation	Environment
1	Medium-bedded (10-25 cm), tan, sharp-based, structureless, fine-grained sandstone with root traces and subordinate, relict ripple cross-laminations. Little to no organic material present.	Channelized, traction transport in the lower part of the lower flow regime followed by pedogenesis.	Floodplain (uppermost point bar)
2	Thick-bedded (25-100 cm), tan and gray, sharp-based, trough and planar-tabular cross-bedded, very fine- to fine-grained sandstone with broad, low-angle inclined beds (lateral accretion sets) and numerous mudstone rip-up clasts near the base of sandstone units. Little to no organic material present.	Channelized, traction transport in the upper part of the lower flow regime with seasonal discharge fluctuation.	Meandering Fluvial (lower point bar/thalwag)
3	Medium- to thick-bedded (10-100 cm), tan, laterally discontinuous, sharp-based, trough cross-stratified and ripple cross-laminated, fine to very-fine grained sandstone with subordinate carbonaceous mud drapes on cross-beds.	Channelized, traction transport in the upper and lower parts of the lower flow regime with seasonal influx of organics.	Meandering Fluvial (mid point bar)
4	Very thin-bedded (1-3 cm), tan to brown, ripple cross-laminated very fine- to fine-grained sandstone.	Channelized, traction transport in the lower flow regime.	Meandering Fluvial (upper point bar)
5	Medium-bedded (10-25 cm), tan and brown, semi-continuous beds of climbing-ripple cross-laminated,very fine- to fine-grained sandstone with subordinate trough cross-beds.	Traction transport in the lower flow regime with episodic but high sediment influx.	Meandering Fluvial (chute channel)
6	Medium-bedded (10-25 cm), tan and brown, broadly lenticular beds of planar-tabular and wedge-planar cross-bedded, fine- to medium-grained sandstone.	Channelized, traction transport in the lower flow regime.	Meandering Fluvial (mid-lower point bar)

observations suggest that Facies C1 and C4 were part of the upper to uppermost point-bar deposits (Table 3). Facies C5 is unique because it predominantly consists of climbing-ripple cross-laminated sandstone, with some subordinate trough cross-beds, and tends to cut upper and upmost point-bar deposits (Facies C1, C4), suggesting that C5 is part of a chute channel or crevasse splay environment. Facies C6 records deposition within the fastest, deepest part of meandering fluvial channels (i.e., thalwag); this interpretation is supported by the high net sand, thicker bedding (25-100 cm), rip-up clasts at the base of sandstone bodies, high-energy traction transport sedimentary structures such as trough cross-bedding, and cross-bedding that is nearly 2x the height of any other facies (Table 3).

Reservoir Characteristics

Potential reservoirs in the sandstone lithofacies assemblage (Assemblage C) have relatively few heterogeneities and simple external geometries. Although the facies in Assemblage C tend to be vertically and laterally amalgamated, they are typically high net-to-gross sand, have thicker bed sets, and generally cluster in sand-rich successions. Externally, the sandstone bodies range from 500-2000 m in width due to lateral amalgamation, and are generally between 2-10 m in thickness. Internally, the sand bodies contain moderate- to well-sorted, stratified sandstone that are superimposed on broad (10's of m), low-angle, inclined bed-sets. Although the sandbodies have a relatively simple external geometry and relatively few mud baffles, fluid flow will likely follow the inclined bed sets (lateral accretion sets). In addition, these sandstones, especially Facies C2 and C3, are likely to fracture due to their longer lateral extent (up to 2000 m) and homogeneity.

The sandstone lithofacies (Assemblage C) are easily identified in the GR curve as thicker (2-10 m thick) intervals with sharp-based, blocky GR motif with relatively low GR response (< 35 cps). A good example of this is between 248-260 m in the Thompson Canyon Section (Figure 5B, 8, 9). However, GR responses for sandstones in the upper part of the Farrer Formation are 5-10 cps higher than the sandstones in the middle and lower parts of the Farrer Formation due to the roughly 10% increase in detrital k-feldspar. Boundaries between channel-sandstone bodies are usually marked by a slight increase in GR response, nearing 35 cps, due to the increased organic content and decrease in grainsize.

PALEOCURRENT ANALYSIS

Paleocurrents were measured every 10-25 m whenever possible. Planar-tabular cross-beds, wedge-planar cross-beds, ripple crests, ripple cross-lamination, clast imbrications, parting lineations, tool marks and flute casts were measured in this study. At each locality a minimum of 3-5 measurements were taken in the field, rotated for structural dip if the bedding attitude was >15 deg and plotted on rose diagrams using StereoWin 7.0. The rose diagrams are displayed on the right hand side of stratigraphic profiles (Figure 5 and Appendix A).

Paleocurrent data from the lower part of the Farrer Formation suggest that river systems were flowing toward the northeast. However, the uppermost part of the Farrer Formation tends to have paleocurrents with a more northerly orientation. The shift in paleocurrents from more easterly to northerly direction is consistent with previous studies (Lawton, 1983). Previous workers have suggested that the change in paleocurrent

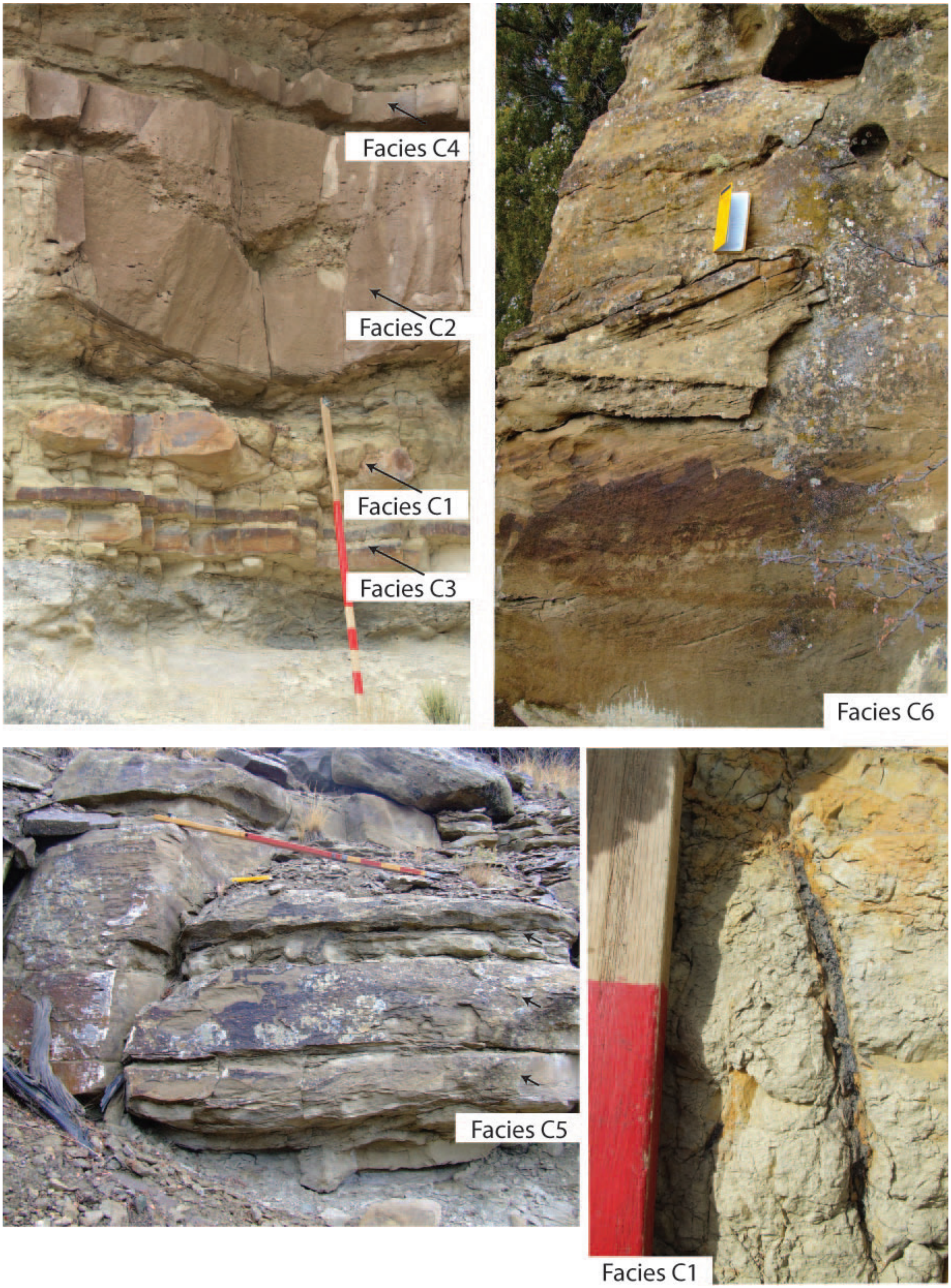

Figure 7. *Examples of facies constituting the sandstone facies assemblage.*

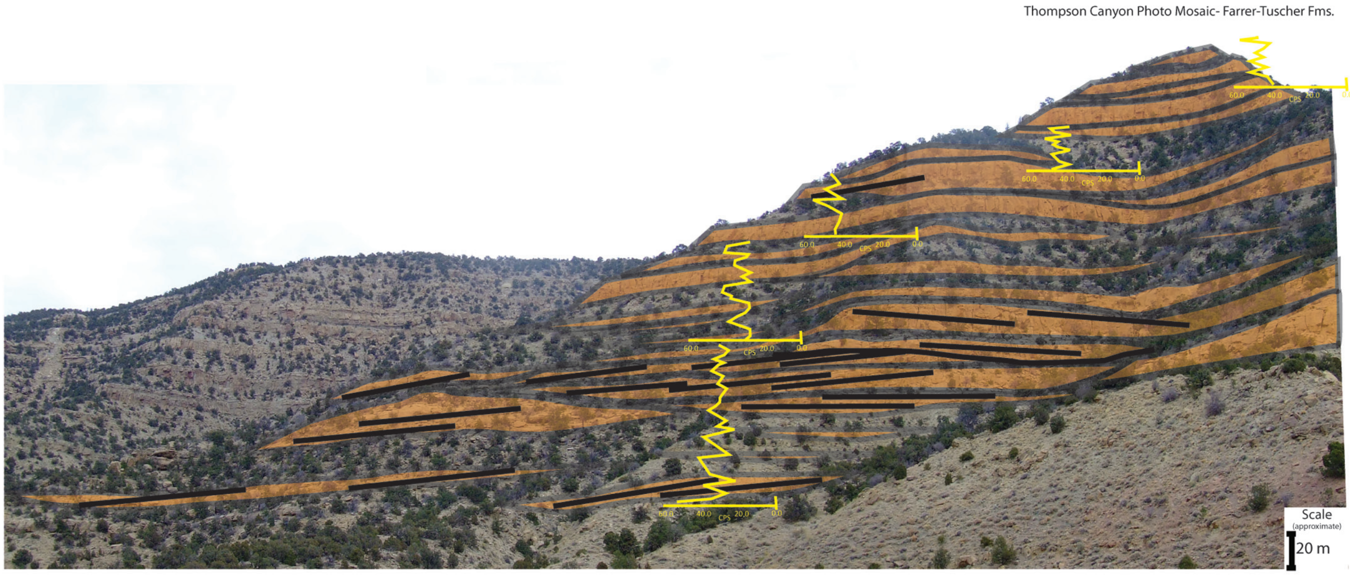

__Figure 8.__ Photomosaic of the Farrer Formation at Thompson Canyon showing channel architecture with superimposed gamma-ray curve (yellow) measured with multispectral GR spectrometer. Click here to view enlarged figure. Raw GR spectrometer data are provided in Appendix B.

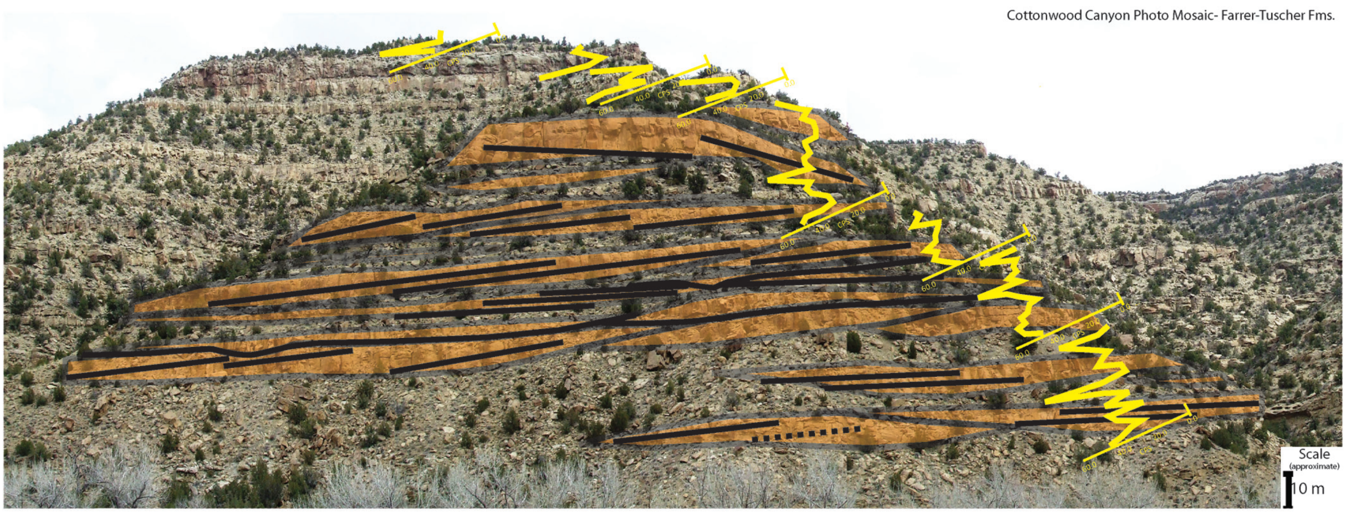

__Figure 9.__ Photomosaic of the Farrer Formation at Cottonwood Canyon showing channel architecture with superimposed gamma-ray curve (yellow) measured with multispectral GR spectrometer. Click here to view enlarged figure. Raw GR spectrometer data are provided in Appendix C.

direction was caused by uplift of the San Rafael Swell, a Laramide structure that was thought to have been active from the latest Cretaceous (~77 Ma) to early Paleogene (DeCelles, 2004; Aschoff, 2008). More detailed correlation and additional paleocurrent data in the vicinity of the San Rafael Swell are needed to discern whether this structure was responsible for the paleocurrent shift.

REGIONAL CORRELATION

Discovery of two flooding surfaces within the Farrer and Price River Formations allowed the regional correlation of the two units from Willow Creek (near Price, UT) to the UT-CO state line. Numerous unconformities are present in the Farrer-Price River interval and were difficult to trace laterally; hence, flooding surfaces and formation tops, rather than sequence boundaries, were mainly used to construct the correlation (Plates 1 and 2). Moreover, unconformities become more numerous and clustered in the vicinity (+/- 20 km) of the San Rafael Swell. In the field, flooding surfaces were identified using evidence tidal, brackish and/or marine influence including marine- to-brackish trace fossils, flaser- and lenticular-bedding and bi-directional ripple cross-lamination. In the subsurface, flooding surfaces were identified by the presence of a higher-than-average gamma-ray response within a thick shale-rich interval (Figure 4 and Figure 5).

Both flooding surfaces are more pronounced in the eastern part of the Uinta Basin; this is likely because the eastern margin was more frequently influenced by sea-level fluctuations in the nearby Western Interior Seaway. The lower flooding surface is better defined and more regionally extensive than the upper flooding surface in the Farrer Fm. The lower flooding surface (Flooding Surface 1) is recognized from Horse Canyon to the UT-CO state line; it is generally marked by a non-waltherian facies shift, where meandering fluvial strata are overlain by outer or inner estuarine facies or tidally influenced fluvial facies. Facies translation across this surface decreases westward to Price, where it is extremely subtle and tends to occur in the thick covered intervals in the Price River Formation. The upper flooding surface is generally observed east of Green River, UT where it is marked by a thin interval (<5 m thick) where flaser-bedded sandstones with bi-directional current indicators and carbonaceous shales intertongue with meandering fluvial facies. In the subsurface, flooding surfaces are found within low net-to-gross sand intervals where channel sands tend to be thinner and more isolated. Within the low net-to-gross intervals flooding surfaces had higher GR response compared to fluvial sandstones, and slightly lower GR response compared to floodplain sandstones with a characteristic "spiky" character and higher organic content.

Stratigraphic stacking patterns and fluvial architecture provide some insight into regional base-level changes, and can be used as a rough tool for correlating non-marine successions (Shanley and McCabe, 1991; Olsen and others., 1995; Martinson and others., 1999). In the Farrer and Price River Formations, there are two packages of fluvial strata that become thicker, sandier and progressively more amalgamated (Figure 5). These two coarsening-up packages are bounded by the two flooding surfaces. Using the surfaces and stacking patterns two genetic sequences can be defined- one in the lower part of the Farrer –Price River interval and one in the upper part of the Farrer-Price River interval. Genetic sequences (Sensu Galloway, 1989) are used in favor of depositional sequences in this study because flooding surfaces are easier to identify and more extensive than unconformities, or sequence boundaries.

Dickinson and others. (1986) and later, Lawton and others. (2003) suggested that detrital sandstone composition can be a useful tool for building and corroborating stratigraphic correlations. The present study adopted this concept but used field-estimated detrital modes instead of thorough petrographic investigation due to the limited time for this study. However, field-estimated composition showed an up-section increase in feldspar (probably k-spar, but no thin-sections were examined) in sandstones of the upper Farrer Formation; this increase in feldspar corresponded to an up-section increase in the total GR response of sandstones. The correlation presented here (Plates 1 and 2) is consistent with this stratigraphic pattern in sandstone composition.

In general, stratigraphic stacking patterns and stratigraphic patterns in detital composition are consistent with the correlation of the two flooding surfaces in the Farrer and Price River Formations. Although this study presents several new tools to correlate the Farrer-Price River interval, much more work is needed to fully understand the connection of depositional systems and 3-dimensional distribution of sand. Additional work is needed in several key areas: (1) more detailed analysis of the regional sequence stratigraphy that uses the two key flooding surfaces, as well as higher-order surfaces between them, (2) the 3-dimensional perspective of this correlation, (3) detailed, regional subsurface mapping of specific facies and (4) palynology to constrain the correlation.

CONCLUSIONS

Subsurface stratigraphic correlations in the upper Mesaverde Group are challenging due to the similarity of log facies and abundance of non-marine deposits that tend to have more subtle flooding surfaces. As a result, previous workers primarily used formation tops and "net-to-gross" patterns to correlate; such correlations can lead to oversimplified models of depositional systems, their connectivity and facies distribution. The pilot study presented here used flooding surfaces, regional unconformities, detailed lithofacies, facies stacking patterns/architecture, sandstone composition and paleocurrents from outcrop data to improve the regional, subsurface correlation. Two flooding surfaces discovered during study were particularly useful for constructing the regional correlation, and making the critical link from the outcrop to the subsurface. Flooding surfaces were identified in outcrop by the presence of tidal- and marine-influenced units that suggest incursion of brackish to open-marine conditions into predominantly fluvial successions; they can be identified by their higher GR response compared to fluvial sandstones, and slightly lower GR response compared to floodplain sandstones with a characteristic "spiky" character and higher organic content. In addition, an up-section increase in detrital feldspar (probably k-spar, but no thin-sections were examined) in sandstones of the upper Farrer Formation correspond to an up-section increase in the total GR response of sandstones.

Outcrop analysis and correlation of outcrop and subsurface data suggest that subtle flooding surfaces are the most useful tools for correlating long distances (> 50 km) in the Price River and Farrer Formations. These flooding surfaces provide the best time-lines. Changes in fluvial stacking pattern, from clustered to isolated channel bodies, allow us to identify stratigraphic zones that may contain flooding surfaces. Careful examination of the GR and conductivity within these suspect zones helps to identify key flooding surfaces. Locally, unconformities are useful for correlation purposes but they are very difficult to follow for more than a few kilometers. The unconformities become more numerous and clustered near the San Rafael Swell; these unconformities appear to become conformable with distance away from the San Rafael Swell and may locally act as stratigraphic traps. It is possible that these unconformities form part of a large-scale growth-strata package on the margins and crest of the San Rafael Swell. However, this is mere speculation at this early stage in the project ; much more detailed stratigraphic analysis in the San Rafael Swell area is needed to fully understand the extent, character and genesis of these unconformities.

A wide range of depositional lithofacies were described from the Price River and Farrer Formations. These included: sandy meandering fluvial channels, floodplain mudstone, sandy crevasse splay deposits, tidally influenced fluvial and estuarine facies. Previously, tidally influenced facies were not recognized in the Farrer-Price River interval. However, these rare tidal facies were key to identifying flooding surfaces and constructing the correlation.

Partitioning of depositional facies was recognized within the Price River and Farrer Formations. The lower part (generally 75-100 m) of the interval is a low net-to-gross sand succession consisting of more isolated channel bodies, fewer crevasse splay deposits and less developed paleosols (thinner units with scare root traces and peds). Two important flooding surfaces are found within this lower stratigraphic interval. By contrast, the upper part of the Price River-Farrer succession is a higher net-to-gross interval with thicker and more amalgamated channel bodies, more crevasse splay deposits and better developed paleosols (thicker units with large, fully preserved root traces). Geographically, sandstone-rich intervals are more abundant on the distal flanks (>20 km) of the San Rafael Swell. Paleocurrents are highly variable, but are generally north- to northeast-directed currents that become more northerly in the vicinity of the San Rafael Swell.

Preliminary paleocurrent data from this study is consistent with previous work that suggests the San Rafael Swell deflected fluvial systems northward. In addition, the San Rafael Swell may have formed semi-regional unconformities along its crest during phases when uplift exceeded sedimentation. These large-scale syntectonic unconformities may correlate to packages of sediment off the crest of the San Rafael Swell, perhaps to the north or northeast. Moreover, episodic uplift of the San Rafael Swell may have controlled regional accommodation patterns that ultimately influenced fluvial architecture and sand distribution in the Uinta Basin. Uplift of the San Rafael Swell would likely shift depositional loci further toward the north or south of the San Rafael Swell.

This pilot study identified two key surfaces that were used to improve correlation and provide better timelines in the Farrer and Price River Formations. The correlation presented here reflects better integration of outcrop and subsurface data, and provides some insight into the log characteristics and reservoir potential of facies within this stratigraphic interval. This study is the groundwork for a more detailed regional sequence-stratigraphic correlation in the lower Mesaverde Group that will help us understand the regional connectivity of depositional systems and sand distribution. Future work will include (1) a more detailed analysis of the regional sequence stratigraphy that uses the two key flooding surfaces, and higher-order surfaces between them, (2) a more 3-dimensional perspective of this correlation, (3) additional outcrop GR curves that better define the log characteristics of facies constituting this interval, (4) detailed, regional subsurface mapping of specific facies and (5) palynology.

REFERENCES

Aschoff, J.L., 2008, Controls on clastic wedge and growth strata development in foreland basins: Examples from Cretaceous Cordilleran Foreland Basin strata, USA, PhD thesis, University of Texas at Austin, Austin, TX 179 p.

Bump, A.P. and Davis, G.H., 2003, Late Cretaceous-early Tertiary Laramide deformation of the northern Colorado Plateau, Utah and Colorado: Journal of Structural Geology, v. 25, p. 421-440.

Cobban, W.A., Walaszczyk, I., Obradovich, J.D., and McKinney, K.C., 2006, A USGS zonal table for the upper Cretaceous middle Cenomanian-Maastrichtian of the upper western Interior of the United States based on ammonites, inoceramids, and radiometric ages: U.S. Geological Survey Open-File Report 2006-1250, 46 p., 1 sheet.

DeCelles, P.G., 2004, Late Jurassic to Eocene evolution of the Cordilleran Thrust Belt and foreland basin system, western U.S.A: American Journal of Science, v. 304, p. 105-168.

Dickinson, W.R., and Snyder, W.S., 1978, Plate tectonics of the Laramide orogeny, *in* Matthews, V., III, ed., Laramide folding associated with basement block faulting in the western United States: Geological Society of America Memoir 151, p. 355–366.

Dickinson, W.R., Lawton, T.F. and Inman, K.I., 1986, Sandstone detrital modes, central Utah foreland region: stratigraphic record of Cretaceous-Paleogene tectonic evolution: Journal of Sedimentary Petrology, v. 56, p. 276-293.

Fisher, D.J., Erdmann, C.E., and Reeside, J.B., 1960, Cretaceous and Tertiary formations of the Book Cliffs, Carbon, Emery and Grand Counties, Utah and Garfield and Mesa Counties, Colorado: USGS Professional Paper 332, 80 p.

Fouch, T. D., Lawton, T. F., Nichols, D. J., Cashion,W. B., and Cobban,W. A., 1982, Chart showing preliminary correlation of major Albian to middle Eocene rock units from the Sanpete Valley in central Utah to the Book Cliffs in eastern Utah, *in* Nielson, D.L., editor, Overthrust belt of Utah, symposium and field conference: Utah Geological Association Publication 10, p. 267–272.

Fouch, T.D., Nuccio, V.F., Anders, D.E., Rice, D.D., Pitman, J.K., and Mast, R.F., 1994, Green River petroleum system, Uinta Basin, Utah, USA; *in* Magoon, L.B., and Dow, W.G., editors, The petroleum system from source to trap: American Association of Petroleum Geologist Memoir, vol. 60, pp 399-421.

Galloway, W.E., 1989, Genetic stratigraphic sequences in basin analysis I: architecture and genesis of flooding-surface bounded depositional units: American Association of Petroleum Geologists Bulletin, v. 73, p. 125-142.

Guiseppe, A. C., and Heller, P. L., 1998, Long-term river response to regional doming in the Price River Formation, central Utah: Geology, v. 26, p. 239–242.

Hettinger, R.D., and Kirschbaum, M.A., 2002, Stratigraphy of the Upper Cretaceous Mancos Shale (upper part) and Mesaverde Group in the southern part of the Uinta and Piceance basins, Utah and Colorado: USGS Geologic Investigations Series I-2764, 21 p.

Hintze , L.F., Willis, G.C., Laes, D.Y., Sprinkel, D.A., and Brown, K.D., 2000, Digital geological map of Utah: Utah Geological Survey Map 179DM, scale 1:500,000.

Lawton, T. F., 1983, Late Cretaceous fluvial systems and the age of foreland uplifts in central Utah, *in* Lowell, J. D., ed., Rocky Mountain foreland basins and uplifts: Denver, Rocky Mountain Association of Geologists, p. 181–199.

Lawton, T.F., 1986, Fluvial systems of the Upper Cretaceous Mesaverde Group and Paleocene North Horn Formation, central Utah; a record of thin-skinned to thick-skinned deformation in the foreland region, *in* Peterson, J.A., eds., Paleotectonics and sedimentation in the Rocky Mountain region, United States: AAPG Memoir 41, p. 423-442.

Lawton, T.F., Pollock, S.L. and Robinson, R.A.J., 2003, Integrating sandstone petrology and nonmarine sequence stratigraphy: Application to the Late Cretaceous fluvial systems of southwestern Utah, U.S.A: Journal of Sedimentary Research, v.73, p.389-406.

Martinson, O.J., Ryseth, A., Helland-Hansen, W., Flesche, H., Torkildsen, H., Torkildsen, G. and Idil, S., 1999, Stratigraphic base level and fluvial architecture: Ericson Sandstone (Campanian), Rock Springs Uplift, SW Wyoming, USA: Sedimentology, v. 46, p. 235-259.

Olsen, T., Steel, R., Hogseth, K., and Roe, S. L., 1995, Sequential architecture in a fluvial succession: Sequence stratigraphy in the Upper Cretaceous Mesaverde Group, Price Canyon, Utah: Journal of Sedimentary Research, v. B65, p. 265–280.

Shanley, K.W., and McCabe, P.S., 1991, Predicting faceis architecture through sequence stratigraphy; an example from the Kaiparowits Plateau, Utah: Geology, vol. 19, no. 7, pp. 742-745.

Spieker, E.M., 1946, Late Mesozoic and early Cenozoic history of central Utah: U.S. Geological Survey Professional Paper 205-D, p. 117-161.

APPENDICES

APPENDIX A

Stratigraphic columns collected in this study.

Explanation

Sedimentary Structures and Fabrics

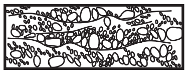
Clast-supported, low-angle stratified, locally imbricated, polymict, cobble conglomerate

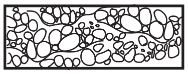
Clast-supported, disorganized, monomict, cobble-boulder conglomerate

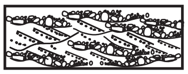
Clast-supported, trough cross-stratified, and low-angle stratified, pebble-cobble conglomerate


Accretion sets (lateral and vertical accretion not distinguished)

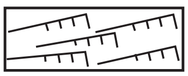
Current ripple cross-lamination

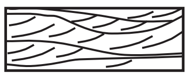
Trough cross-bedding

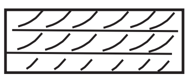
Planar-tabular cross-bedding

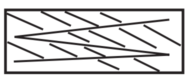
Wedge-planar cross-bedding

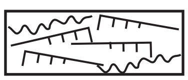
Bi-directional ripple cross-lamination with mud drapes

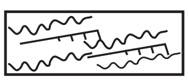
Flaser and lenticular bedding

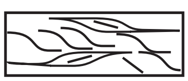
Sigmoidal cross-bedding

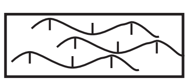
Hummocky cross-bedding


Bioturbation and hummocky cross-bedding


Ophiomorpha- and *Thalassinoides*- burrowing

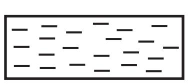
Shale and mudstone

Other Symbols and Notation

Sequence Boundary (dashed where uncertain)

Transgressive Surface (dashed where uncertain)

Maximum Flooding Surface (rarely preserved)

Rose diagram of paleocurrent data

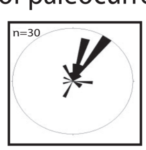

Grain-size scale

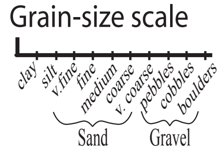

Cottonwood Canyon Section (CC-01)

Appendix A

Floy Canyon Section (FlC-01)

Appendix A

Green River Section (GrF-01)
Burrows
Wood present
Parting lineations
Concretions
Concretions locally
meters
cl st vf f m c vc g p c b
Mud
Sand
Gravel

Appendix A

Hays Canyon Section (HAF-01)

Appendix A

Horse Canyon Section (HCF-01)

Appendix A

Nine Mile Canyon Section (NMF-01)

Appendix A

San Arroyo Canyon Section (SAF-01)

Appendix A

San Arroyo Canyon Section (SAF-01)

Appendix A

Turtle Canyon Section (TCF-01)

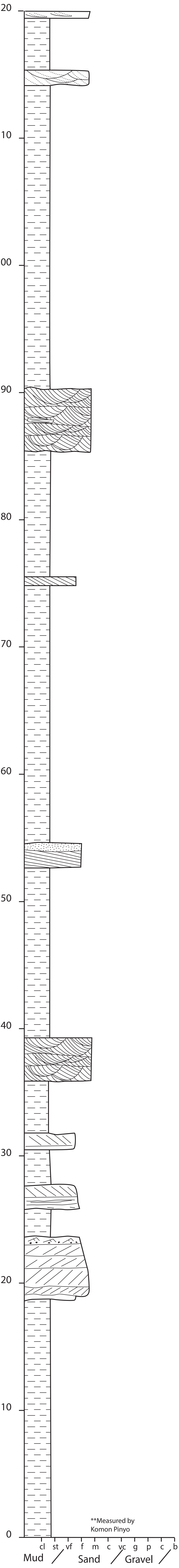

Willow Creek Section (WCF-01)

APPENDIX B

Raw GR spectrometer assay data for the Thompson Canyon locale.

Appendix B

GR Spectrometer Raw Assay Data- Thompson Canyon Section

ID	Meters	cps	Date	Time	Temp. C	Total[ppm]	Total[cpm]	Total [cps]	K[ppm]	K[cpm]	U[ppm]	U[cpm]	Th[ppm]	Th[cpm]	Dose	Dose units
151	4.5	53.3	11/26/08	12:31:36	10.6	373.3	3196.1	53.3	2.16	201.8	3.66	64.1	37.19	69.5	148.34	nGy/h
152	6	34.4	11/26/08	12:36:56	11.4	241.1	2064.1	34.4	1.35	132.6	5.03	45.9	17.84	33.6	93.06	nGy/h
164	9	26.4	11/26/08	12:44:34	12.2	185.2	1585.5	26.4	1.28	109.8	3.28	30.9	12.39	23.3	67.91	nGy/h
165	13.5	38.8	11/26/08	12:59:45	12.9	271.7	2326	38.8	1.77	159.1	5.21	48.5	19.28	36.3	103.35	nGy/h
167	16.5	21.1	11/26/08	13:08:04	13	148.1	1268.3	21.1	0.85	89.6	4.51	34	10.33	19.6	63.47	nGy/h
169	18.5	35.2	11/26/08	13:13:23	13	246.8	2113	35.2	1.39	144	6.82	53.7	17.46	33.1	102.25	nGy/h
172	28.5	41.4	11/26/08	13:19:03	13	290.3	2485.5	41.4	1.82	162.8	4.12	48.5	23.23	43.5	108.85	nGy/h
174	30.5	24.8	11/26/08	13:26:41	13.2	173.9	1488.6	24.8	1.21	99.9	1.52	25.7	14.71	27.4	63.7	nGy/h
175	40	38.8	11/26/08	13:44:11	13.4	272.2	2330.2	38.8	2.62	207.8	5.89	49.6	17.66	33.1	113.85	nGy/h
176	43	21.8	11/26/08	13:48:34	13	152.5	1305.6	21.8	1.03	90.1	3.03	26.2	9.61	18.1	55.84	nGy/h
178	45.5	31.3	11/26/08	13:55:42	13	219.4	1878.8	31.3	1.69	147.1	5.89	42.8	12.28	23.3	87.17	nGy/h
180	47.5	28.6	11/26/08	14:03:28	13.4	200.2	1714	28.6	1.58	132	4.53	35.5	11.52	21.7	76.28	nGy/h
181	48.5	26.4	11/26/08	14:16:26	14.1	185.1	1584.4	26.4	1.53	131	5.72	37.1	8.39	16	73.74	nGy/h
182	54.5	35.9	11/26/08	14:23:46	14.4	251.9	2156.6	35.9	2.24	183.9	6.13	47.5	15.1	28.5	103.34	nGy/h
184	57	32.1	11/26/08	14:31:27	14	224.8	1924.8	32.1	2.27	177.1	5.27	40.7	12.94	24.3	93.18	nGy/h
185	59	29.8	11/26/08	14:41:05	14.2	208.9	1788.5	29.8	1.34	121.2	3.95	37.1	14.85	27.9	79.01	nGy/h
186	61.5	29.7	11/26/08	14:48:52	14.2	208	1780.8	29.7	1.53	133.6	5.02	39.2	12.59	23.8	81.13	nGy/h
188	65	27.2	11/26/08	15:02:31	14	190.4	1630	27.2	1.35	125.8	7.03	41.2	6.9	13.4	74.46	nGy/h
190	66.5	26.0	11/26/08	15:05:30	13.8	182.3	1561.1	26.0	1.54	122.7	4.05	29.8	8.77	16.5	65.79	nGy/h
191	69	31.0	11/26/08	15:09:02	13.6	217.1	1858.5	31.0	1.59	142.9	6.7	44.3	10.55	20.2	85.55	nGy/h
192	73.5	27.8	11/26/08	15:13:26	13.4	194.9	1668.9	27.8	1.8	141.9	5.11	34	8.18	15.5	73.3	nGy/h
193	76	34.3	11/26/08	15:24:41	12.8	240.2	2056.5	34.3	1.9	155.9	4.23	40.2	16.28	30.5	91.65	nGy/h
195	79.5	30.4	11/26/08	15:27:21	12.8	212.8	1822.2	30.4	1.59	125.3	2.7	29.3	13.29	24.8	71.25	nGy/h
197	81	27.4	11/26/08	15:30:59	12.6	191.7	1641.4	27.4	1.72	134.6	3.12	30.9	13.01	24.3	74.49	nGy/h
198	82.5	32.8	11/26/08	15:54:03	9.8	230.1	1970.4	32.8	1.9	152.8	4.75	37.6	12.37	23.3	84.02	nGy/h
199	85	27.4	11/26/08	16:01:34	11.2	191.8	1641.9	27.4	1.92	146.5	4.73	31.9	7.94	15	72.27	nGy/h
200	87.5	24.9	11/26/08	16:12:12	11.4	174.4	1493.3	24.9	1.89	139.8	3.28	27.8	9.97	18.6	69.37	nGy/h
201	90.5	30.2	11/26/08	16:18:47	11.2	211.9	1814	30.2	1.72	148.6	6.66	42.8	9.46	18.1	84.23	nGy/h
202	93	32.5	11/26/08	16:23:12	11.2	227.9	1951	32.5	1.94	161.6	6.15	43.3	11.74	22.2	90.43	nGy/h
204	95.5	29.6	11/26/08	16:26:35	11.2	207.2	1774.1	29.6	1.91	146.5	3.19	31.9	13.58	25.3	78.89	nGy/h
205	99	29.8	11/26/08	16:29:52	11.3	208.8	1787.5	29.8	1.56	128.9	3.38	33.5	14.08	26.4	76.72	nGy/h
220	103	41.2	11/27/08	10:09:44	9.2	288.8	2472.7	41.2	2.32	195.4	6.23	53.2	19.28	36.3	116.06	nGy/h
223	106	36.6	11/27/08	10:13:20	9.4	256.3	2194.1	36.6	2.53	189.1	3.38	38.1	17.8	33.1	99.41	nGy/h
224	108	32.3	11/27/08	10:15:56	9.6	226.6	1940.4	32.3	2.3	176.1	4.89	38.6	12.69	23.8	90.8	nGy/h
233	110.5	29.8	11/27/08	10:22:47	10.4	209.1	1790.6	29.8	1.86	156.4	6.2	42.8	11.17	21.2	88.06	nGy/h
235	113	30.3	11/27/08	10:30:34	10.6	212.5	1819.1	30.3	1.27	126.9	6.47	45.4	12.19	23.3	84.61	nGy/h
236	115.5	40.2	11/27/08	10:34:09	10.4	281.9	2413.4	40.2	2.01	166.9	3.6	43.3	21.06	39.4	102.64	nGy/h
237	117	39.9	11/27/08	10:40:18	10.6	279.4	2391.9	39.9	2.27	188.1	6.51	49.6	15.36	29	106.48	nGy/h
238	119	44.8	11/27/08	10:42:54	10.5	314	2688.5	44.8	2.64	201.7	4.05	43.4	19.45	36.3	108.96	nGy/h
239	122.5	43.5	11/27/08	10:48:18	10.5	305.1	2612.7	43.5	1.85	177.8	6.4	59.9	23.93	45.1	123.36	nGy/h
241	124.5	29.3	11/27/08	10:49:27	10.4	205.4	1759	29.3	0.9	101	5.74	41.1	11.48	21.9	73.89	nGy/h
243	127.5	34.0	11/27/08	11:05:42	10.2	238.2	2039.3	34.0	1.5	138.8	5.54	44.3	14.77	27.9	89.53	nGy/h
245	129.5	29.1	11/27/08	11:16:59	10.4	204.2	1748.7	29.1	1.97	154.8	4.41	36.1	12.4	23.3	83.15	nGy/h
246	134.5	38.2	11/27/08	11:22:51	10.4	267.8	2292.7	38.2	2.73	207.3	4.47	43.8	18.31	34.2	109.39	nGy/h
247	137	37.8	11/27/08	11:26:40	10.4	264.8	2267.5	37.8	2.26	179.8	5.22	43.3	15.16	28.5	98.74	nGy/h
248	138.5	31.8	11/27/08	11:31:14	10.4	222.6	1905.6	31.8	2.17	162.6	3.45	33.5	13.87	25.9	84.4	nGy/h
249	139.5	30.5	11/27/08	11:36:38	10.5	213.7	1829.5	30.5	2.02	164.2	6.04	41.8	10.92	20.7	88.68	nGy/h
250	145	29.7	11/27/08	11:43:28	10.4	207.9	1780.3	29.7	2.19	161	2.95	30.9	13.63	25.3	81.45	nGy/h
251	151.5	34.2	11/27/08	11:49:22	10.6	239.9	2054.1	34.2	2.14	165.7	4.67	37.6	12.68	23.8	87.44	nGy/h
252	154.5	34.5	11/27/08	12:03:53	10.6	241.8	2070.2	34.5	2.54	183.4	3.75	33.5	12.79	23.8	88.03	nGy/h
253	158.5	32.3	11/27/08	12:25:13	9.8	226.3	1937.7	32.3	2.07	163.6	5.78	39.2	9.83	18.6	84.98	nGy/h

254	163	30.9	11/27/08	12:43:01	9.6	216.6	1854.4	30.9	1.96	157.4	5.32	39.2	11.51	21.7	85.48	nGy/h
255	166.5	38.4	11/27/08	12:47:55	9.2	269.4	2306.5	38.4	2.29	177.7	3.57	39.7	18.32	34.2	98.76	nGy/h
256	169.5	46.5	11/27/08	12:51:45	9.4	325.7	2788.7	46.5	2.36	196	2.71	50.6	30.04	56	126.53	nGy/h
261	170	30.5	11/27/08	13:03:47	9.4	213.5	1827.9	30.5	1.62	135.1	3.64	36.1	15.18	28.5	81.77	nGy/h
262	175	39.8	11/27/08	13:15:02	9.4	278.6	2385.5	39.8	2.37	183.9	3.29	41.3	20.56	38.3	104.23	nGy/h
263	177.5	32.0	11/27/08	13:18:28	9.4	224.6	1922.8	32.0	1.77	137.7	2.27	30.9	16.11	30	78.88	nGy/h
271	180.5	34.6	11/27/08	13:24:19	9.4	242.5	2076.7	34.6	1.77	150.7	3.46	41.2	19.92	37.3	95.62	nGy/h
272	182.5	36.8	11/27/08	13:42:50	10.5	257.8	2207.6	36.8	2.95	207.8	4.63	35	10.84	20.2	92.89	nGy/h
273	186.5	27.4	11/27/08	13:56:08	10.2	191.7	1641.1	27.4	1.87	139	3.55	28	9.2	17.2	68.51	nGy/h
275	189	32.7	11/27/08	13:58:58	10.1	229	1961.1	32.7	1.52	145	7.8	49	10.2	19.6	89.77	nGy/h
276	195	36.8	11/27/08	14:16:57	9.2	257.5	2205	36.8	2.27	181.3	5.02	43.8	16.28	30.5	100.87	nGy/h
277	198.5	26.7	11/27/08	14:20:26	9.3	187.4	1604.1	26.7	1.78	144	5.11	36.1	9.84	18.6	77.58	nGy/h
278	201.5	33.7	11/27/08	14:24:10	9	235.9	2019.6	33.7	1.99	153.3	1.75	33.5	20.05	37.3	89.47	nGy/h
279	203	35.9	11/27/08	14:28:14	9	251.7	2155.2	35.9	1.46	143.5	3.78	49	24.86	46.6	106.64	nGy/h
280	205.5	33.4	11/27/08	14:30:41	9	233.8	2002	33.4	1.55	136.2	2.77	39.2	20.77	38.8	91.35	nGy/h
281	208	40.6	11/27/08	14:35:37	9.2	284.3	2434.3	40.6	1.93	167.3	5.09	48	19.29	36.2	104.8	nGy/h
282	211	26.2	11/27/08	14:43:05	9.2	183.5	1571.4	26.2	1.43	116.5	2.7	29.3	13.28	24.8	69.14	nGy/h
283	213.5	35.1	11/27/08	14:47:33	9.4	245.7	2103.7	35.1	2.37	181.8	5.08	40.2	13.24	24.8	94.18	nGy/h
284	216.5	37.6	11/27/08	14:52:02	9.2	263.5	2255.7	37.6	1.77	154.3	4.45	44.4	18.75	35.2	97.88	nGy/h
285	218	27.2	11/27/08	14:56:27	9	190.3	1629	27.2	1.32	121.2	5.3	38.6	11.16	21.2	76.06	nGy/h
286	222.5	30.7	11/27/08	15:02:19	9.2	214.9	1840.3	30.7	1.7	134.6	1.84	31.4	18.07	33.6	80.9	nGy/h
287	226	40.0	11/27/08	15:10:14	9.4	280.6	2402.3	40.0	1.68	166.9	7.91	59.4	17.98	34.2	113.32	nGy/h
288	229.5	30.8	11/27/08	15:35:47	9	215.6	1846	30.8	1.57	142.4	7.12	44.9	9.42	18.1	84.55	nGy/h
289	233.5	40.1	11/27/08	15:39:29	9	281.1	2407	40.1	2.13	181.4	6.12	50.6	17.59	33.1	108.46	nGy/h
290	236.5	32.6	11/27/08	15:40:09	9	228.4	1955.8	32.6	1.71	151	6.95	45.3	10.37	19.8	88.06	nGy/h
292	239	37.1	11/27/08	15:46:19	9	260	2226.4	37.1	1.97	171.5	6.28	49.5	16.17	30.5	103.52	nGy/h
293	242	32.6	11/27/08	15:49:48	8.8	228.1	1953.3	32.6	2.32	177.1	5.28	38.6	11.28	21.2	89.39	nGy/h
294	245.5	29.4	11/27/08	15:53:51	8.6	205.8	1762.1	29.4	1.58	139.8	6.4	42.3	10.02	19.1	82.34	nGy/h
295	247.5	45.6	11/27/08	15:56:39	8.4	319.6	2736.7	45.6	2.43	217.2	9.46	66.2	17.7	33.7	130.88	nGy/h
296	249	36.1	11/27/08	15:59:37	8.5	252.7	2163.7	36.1	2.37	187	5.29	44.4	15.72	29.5	102.02	nGy/h
297	252	36.4	11/27/08	16:02:40	8.5	255	2183.4	36.4	2.77	202.2	4.81	38.5	12.86	24	97.03	nGy/h
298	255	36.9	11/27/08	16:06:31	8.6	258.4	2212.1	36.9	2.75	205.7	5.22	42.3	14.39	26.9	103.01	nGy/h
299	258	32.5	11/27/08	16:11:04	8.9	227.7	1949.7	32.5	2.18	169.3	3.93	38.1	15.78	29.5	92.38	nGy/h
300	260.5	44.0	11/27/08	16:15:06	8.9	308.2	2638.8	44.0	1.7	186.1	11.91	74.5	15.25	29.5	128.03	nGy/h
301	262.5	57.7	11/27/08	16:19:00	8.6	404.1	3460.1	57.7	2.91	263.1	11.95	81.8	20.95	39.9	159.45	nGy/h
302	263.5	30.8	11/27/08	16:22:00	8.8	215.6	1846	30.8	2.37	170.4	4.92	31.4	6.87	12.9	76.17	nGy/h
303	266	39.9	11/27/08	16:26:04	8.6	279.4	2392.5	39.9	2.63	213	7.49	53.7	15.07	28.5	115.72	nGy/h
304	271	35.2	11/27/08	16:30:32	8.8	246.5	2110.8	35.2	2.1	168.9	5.81	41.8	11.78	22.2	90.81	nGy/h
305	273.5	42.3	11/27/08	16:34:54	8.9	296.3	2536.6	42.3	2.43	207.9	8.56	58.9	15.26	29	119.35	nGy/h
308	275	30.5	11/27/08	16:36:41	8.9	213.6	1828.5	30.5	1.69	141.6	5.64	38.3	9.69	18.4	78.87	nGy/h
309	278	29.3	11/27/08	16:38:59	8.8	205	1755.4	29.3	1.67	141.4	5.87	39.2	9.51	18.1	79.34	nGy/h

APPENDIX C

Raw GR spectrometer assay data for the Cottonwood Canyon locale.

Appendix C

GR Spectrometer Raw Assay Data- Cottonwood Canyon Section

ID	Meters	cps	Date	Time	Temp. C	Total[ppm]	Total[cpm]	Total [cps]	K[ppm]	K[cpm]	U[ppm]	U[cpm]	Th[ppm]	Th[cpm]	Dose	Dose units
312	0.5	39.15	3/7/09	11:02:08	29.9	274.3	2348.7	39.15	1.36	156.5	9.44	65.6	17.3	33.1	115.64	nGy/h
313	3.5	32.06	3/7/09	11:07:06	29.9	224.6	1923.3	32.06	1.61	141.6	4.43	41.6	16.66	31.3	89.98	nGy/h
314	5.5	25.33	3/7/09	11:11:01	29.9	177.5	1519.7	25.33	1.28	118.1	4.68	37.6	12.58	23.8	76.07	nGy/h
315	8.5	18.67	3/7/09	11:14:40	29.9	130.8	1120.2	18.67	0.88	78.6	3.59	24.1	5.95	11.4	47	nGy/h
316	11.5	32.31	3/7/09	11:20:29	29.9	226.4	1938.3	32.31	1.81	147.1	4.71	37.1	12.09	22.8	81.88	nGy/h
317	13	35.58	3/7/09	11:23:55	29.9	249.4	2135	35.58	2.27	178.7	5.61	42.3	12.92	24.3	94.92	nGy/h
318	15.5	15.41	3/7/09	11:27:58	29.9	108	924.7	15.41	0.79	64.6	1.65	16.4	6.89	12.9	37.88	nGy/h
319	17.5	36.36	3/7/09	11:36:11	29.9	254.8	2181.5	36.36	2.24	182.4	5.02	45.9	17.94	33.6	104.93	nGy/h
320	19	21.75	3/7/09	11:39:01	29.9	152.4	1305.1	21.75	0.93	89.6	3.71	30.4	10.38	19.6	60.32	nGy/h
321	23	36.59	3/7/09	11:41:59	29.9	256.4	2195.4	36.59	1.95	171.5	6.05	50.6	17.85	33.6	106.39	nGy/h
322	26.5	68.63	3/7/09	11:45:26	29.9	480.9	4117.5	68.63	3.44	317.9	15.12	102.7	25.84	49.3	196.65	nGy/h
323	27	36.41	3/7/09	11:49:26	29.9	255.2	2184.7	36.41	2.28	180.9	4.41	42.8	17.71	33.1	101.54	nGy/h
324	29.5	20.33	3/7/09	11:53:21	29.9	142.4	1219.6	20.33	1.3	95.7	1.55	18.4	8.89	16.5	49.42	nGy/h
325	33	23.11	3/7/09	11:58:13	29.9	161.9	1386.5	23.11	1.27	104.1	3.22	26.7	9.35	17.6	59.29	nGy/h
326	34.5	36.48	3/7/09	12:08:43	29.9	255.6	2188.8	36.48	2.05	173	6.83	47.5	12.54	23.8	97.74	nGy/h
327	37.5	30.32	3/7/09	12:12:02	29.9	212.5	1819.1	30.32	1.73	138.3	4.42	34	10.71	20.2	75.41	nGy/h
328	40	28.17	3/7/09	12:14:40	29.9	197.4	1690.1	28.17	1.89	148.1	4.68	34.5	10.16	19.1	77.55	nGy/h
329	44	38.48	3/7/09	12:19:03	29.9	269.6	2308.7	38.48	1.78	164.3	5.54	52.2	20.92	39.4	109.73	nGy/h
330	46	53.93	3/7/09	12:21:47	29.9	378	3236	53.93	3.5	267.6	5.37	57.9	26.13	48.7	145.29	nGy/h
331	48	31.75	3/7/09	12:28:06	29.9	222.5	1905.1	31.75	2.44	176.1	3.99	32.4	11.1	20.7	83.4	nGy/h
332	50.5	24.13	3/7/09	12:36:33	29.9	169.1	1447.6	24.13	1.57	121.2	3.56	27.2	8.53	16	62.82	nGy/h
333	54.5	34.21	3/7/09	12:44:44	29.9	239.8	2052.8	34.21	2.05	171.4	6.45	46.4	13.12	24.8	97.12	nGy/h
334	56.5	38.21	3/7/09	12:56:20	29.9	267.8	2292.7	38.21	2.63	202.1	4.59	44.4	18.29	34.2	108.61	nGy/h
335	59	32.74	3/7/09	12:59:21	29.9	229.4	1964.2	32.74	2.13	165.2	3.31	37.1	17.2	32.1	92.16	nGy/h
336	62	34.68	3/7/09	13:02:51	29.9	243	2080.7	34.68	1.94	159	5.24	41.2	13.46	25.3	90	nGy/h
337	67	29.85	3/7/09	13:07:48	29.9	209.2	1791.2	29.85	1.83	141.9	3.73	31.9	11.6	21.7	75.47	nGy/h
338	69	27.79	3/7/09	13:13:26	29.9	194.7	1667.3	27.79	1.42	122.2	3.76	34.5	13.49	25.3	75.35	nGy/h
339	70	23.65	3/7/09	13:17:09	29.9	165.7	1419.1	23.65	1.32	112.3	3.78	31.4	10.98	20.7	67.31	nGy/h
340	71.5	32.12	3/7/09	13:39:15	29.9	225.1	1927.4	32.12	1.68	151.7	5.22	46.4	17.58	33.1	97.73	nGy/h
341	76	38.93	3/7/09	13:49:19	11.8	272.8	2335.5	38.93	2.47	187.1	2.2	39	22.77	42.3	105.57	nGy/h
342	77.5	54.47	3/7/09	13:53:07	12	381.7	3268.2	54.47	3.39	269.7	6.85	64.6	26.03	48.7	151.66	nGy/h
343	79.5	29.19	3/7/09	13:56:19	12.1	204.5	1751.2	29.19	1.55	130.5	3.18	35	16.03	30	80.75	nGy/h
344		35.28	3/7/09	13:56:57	12.1	247.2	2116.6	35.28	2.08	192.8	7.49	62	21.56	40.7	125.93	nGy/h
345		29.98	3/7/09	13:57:27	12	210.1	1798.8	29.98	1.77	151.2	7.75	43.2	5.86	11.5	80.99	nGy/h
346		30.43	3/7/09	13:57:56	12	213.3	1826	30.43	1.92	151.2	2.78	34.9	17.38	32.4	87.07	nGy/h
347	81.5	28.93	3/7/09	14:00:58	11.8	202.7	1735.7	28.93	2.14	160.5	3.02	32.9	15	27.9	84.78	nGy/h
348	84.5	47.67	3/7/09	14:05:25	12.2	334.1	2860.2	47.67	3.06	236.4	6.75	53.2	17.39	32.6	123.5	nGy/h
349	87.5	25.81	3/7/09	14:08:08	12.4	180.9	1548.6	25.81	1.53	123.7	2.47	30.4	14.96	27.9	73.76	nGy/h
350	90.5	30.92	3/7/09	14:11:50	13.3	216.7	1855.4	30.92	1.74	135.7	2.73	30.9	14.42	26.9	76.39	nGy/h
351	94.5	36.02	3/7/09	14:17:52	14.6	252.4	2161.1	36.02	2.24	173	3.89	38.6	16.34	30.5	94.37	nGy/h
352	96	32.84	3/7/09	14:23:33	14.8	230.1	1970.4	32.84	2.26	175.6	4.73	39.7	14.08	26.4	93.23	nGy/h
353	97.5	37.87	3/7/09	14:27:42	14.8	265.4	2272.2	37.87	2.18	182.9	4.93	48.9	20.61	38.6	110.85	nGy/h
354	99	31.03	3/7/09	14:36:15	15.8	217.4	1861.6	31.03	1.7	139.8	3.95	36.1	14.06	26.4	81.56	nGy/h
355	101.5	30.21	3/7/09	14:48:46	16.9	211.7	1812.4	30.21	2.2	170.9	5.47	39.2	10.98	20.7	88.03	nGy/h
356	110	27.48	3/7/09	15:03:11	15.6	192.6	1648.7	27.48	2.1	157.9	4.57	32.9	9.36	17.6	77.54	nGy/h
357	105.5	26.66	3/7/09	15:06:26	14.8	186.8	1599.4	26.66	1.84	138.8	3.93	29.3	8.81	16.5	69.16	nGy/h
358	114	40.62	3/7/09	15:10:54	13.8	284.6	2436.9	40.62	2.68	203.2	4.25	42.8	18.33	34.2	107.53	nGy/h
359	120.5	34.70	3/7/09	15:21:14	13	243.2	2082	34.70	2.08	175.6	6.75	48.5	13.66	25.9	100.58	nGy/h
360	123	38.27	3/7/09	15:33:49	11.4	268.2	2295.9	38.27	2.45	194.8	5.55	46.9	16.82	31.6	107.46	nGy/h
361	125	35.43	3/7/09	15:37:45	11.4	248.3	2125.7	35.43	2.17	175.1	5.65	43.8	14.01	26.4	96.74	nGy/h
362	128	25.54	3/7/09	15:40:16	11.4	178.9	1532.1	25.54	1.69	131	2.93	29.3	12.46	23.3	71.61	nGy/h
363	130	19.23	3/7/09	15:45:08	11.3	134.8	1153.9	19.23	1.19	94.7	2.47	22.6	8.83	16.5	52.78	nGy/h
364	131.5	21.63	3/7/09	15:49:13	10.8	151.6	1297.6	21.63	1.57	115.9	2.15	22.6	10	18.6	59.17	nGy/h
365	137.5	31.15	3/7/09	15:53:17	10.8	218.3	1868.9	31.15	1.97	162.1	5.46	42.3	13.44	25.3	91.62	nGy/h

366	141	33.75	3/7/09	15:57:03	10.6	236.5	2024.9	33.75	2.28	168.8	3.75	33.5	12.76	23.8	84.56	nGy/h
367	143	30.72	3/7/09	16:03:03	10.6	215.2	1842.9	30.72	1.98	154.3	4.76	35.5	10.72	20.2	80.59	nGy/h
368	149	53.79	3/7/09	16:10:05	11.3	377	3227.6	53.79	2.77	246.4	8.15	74	28.66	53.9	157.62	nGy/h
369	154	29.17	3/7/09	16:15:06	12	204.4	1750.2	29.17	2.14	159	3.72	31.9	11.63	21.7	79.54	nGy/h
370	167.5	32.95	3/7/09	16:25:46	13	230.9	1976.7	32.95	2.3	179.2	4.65	40.7	15.2	28.5	96.33	nGy/h
371	162	33.63	3/7/09	16:30:05	13.3	235.7	2018	33.63	2.49	186.9	4.42	38.6	14.4	26.9	95.37	nGy/h
372		29.70	3/7/09	16:30:45	13.3	208.1	1782.2	29.70	2.23	155.2	1.41	24.4	14.12	26.1	74.86	nGy/h
373		30.96	3/7/09	16:31:14	13.3	216.9	1857.5	30.96	2.05	155.4	3.26	32.8	14.01	26.1	82.24	nGy/h
374	164	24.90	3/7/09	16:33:36	12.8	174.5	1493.8	24.90	1.53	121.2	3.44	28.8	10.19	19.1	66.17	nGy/h
375	167	24.64	3/7/09	16:39:31	12.5	172.6	1478.1	24.64	1.89	143.4	4.12	30.9	9.36	17.6	72.28	nGy/h
376	169	25.84	3/7/09	16:42:50	12.2	181.1	1550.2	25.84	1.33	118.6	4.57	36.1	11.76	22.2	73.85	nGy/h
377	172.5	30.89	3/7/09	16:45:44	12	216.5	1853.3	30.89	2.22	168.3	3.9	35.5	13.85	25.9	87.56	nGy/h
378	175.5	27.95	3/7/09	16:52:04	11.4	195.9	1677.2	27.95	1.76	135.7	2.19	29.8	15.56	29	76.82	nGy/h
379	179	32.55	3/7/09	16:54:44	11.3	228.1	1952.8	32.55	2.28	170.4	2.97	34.5	16.41	30.5	90.14	nGy/h
380	182.5	45.35	3/7/09	16:58:00	11.3	317.8	2721.2	45.35	3.4	251.4	5.87	49.6	17.76	33.1	124.25	nGy/h
381	183.5	29.94	3/7/09	17:01:06	11.4	209.8	1796.3	29.94	2.11	158.5	3.06	32.4	14.44	26.9	83.18	nGy/h
382	186	26.90	3/7/09	17:06:46	11.6	188.5	1614	26.90	1.81	134.6	1.82	26.7	14.48	26.9	72.54	nGy/h
383	187.5	30.55	3/7/09	17:13:03	12.6	214.1	1833.1	30.55	2.11	160	3.17	34	15.26	28.5	85.89	nGy/h
384	189.5	60.74	3/7/09	17:18:12	13	425.6	3644.1	60.74	3.4	291.7	10.12	82.3	28.07	52.9	175.01	nGy/h
385	191	50.06	3/7/09	17:21:41	13.4	350.8	3003.7	50.06	2.19	209	6.74	69.3	30.05	56.5	146.22	nGy/h
386	193	26.83	3/7/09	17:25:00	13.8	188	1609.8	26.83	1.78	139.3	4.7	32.4	8.48	16	71.66	nGy/h
387	195	41.31	3/7/09	17:29:16	14.1	289.5	2478.6	41.31	2.92	217.7	6.06	44.4	12.97	24.3	106.06	nGy/h
388	196.5	31.79	3/7/09	17:31:44	14.2	222.8	1907.2	31.79	2.35	178.7	6.13	38.6	8.18	15.5	86.12	nGy/h
389	198.5	21.35	3/7/09	17:37:23	14.2	149.6	1281.1	21.35	1.43	112.8	2.41	26.2	11.91	22.2	63.91	nGy/h
390	200	56.29	3/7/09	17:42:00	13.7	394.5	3377.6	56.29	3.9	296.8	7.24	63.6	23.85	44.6	154.6	nGy/h
391	201	29.21	3/7/09	17:44:39	13.6	204.7	1752.3	29.21	2.39	168.3	2.11	27.8	14.25	26.4	81.13	nGy/h
392	203	21.57	3/7/09	17:49:26	13.4	151.2	1294.4	21.57	1.55	122.1	2.55	28.3	13.02	24.3	69.25	nGy/h
393	207	26.55	3/7/09	17:52:13	13	186	1592.7	26.55	1.64	123.2	1.33	25.2	15.05	27.9	69.13	nGy/h
394	211	35.35	3/7/09	17:57:46	12.2	247.7	2120.8	35.35	2.18	181.8	6.36	48.5	15.08	28.5	103.72	nGy/h
395	212.5	31.30	3/7/09	18:00:17	11.8	219.4	1878.2	31.30	1.79	146	5.06	37.6	11.23	21.2	81.08	nGy/h
396	217	61.13	3/7/09	18:03:56	11	428.4	3667.6	61.13	4.27	330.1	9.2	74	24.89	46.7	172.92	nGy/h
397		27.23	3/7/09	18:05:06	10.9	190.8	1633.9	27.23	1.81	129.8	1.32	22.9	13.29	24.6	66.58	nGy/h
398		26.65	3/7/09	18:05:36	10.9	186.8	1599.1	26.65	1.78	130.2	2.05	24.4	11.8	21.9	66.25	nGy/h
399		25.74	3/7/09	18:06:05	10.8	180.4	1544.6	25.74	2.08	149	2.5	26.5	11.81	21.9	72.54	nGy/h
400	218	25.41	3/7/09	18:08:08	10.5	178.1	1524.7	25.41	1.8	136.7	4.4	29.3	7.12	13.4	66.67	nGy/h
401	221.5	22.29	3/7/09	18:12:41	10.1	156.2	1337.3	22.29	1.66	121.1	1.99	22.6	10.57	19.6	61.06	nGy/h

APPENDIX D

Summary of data used to construct Cross Section #1 (Willow Creek to Cottonwood Canyon) and Cross Section #2 (Floy Canyon to the UT-CO state line). Includes names, API, lat/long, cumulative oil and gas and selected formation tops.

Appendix D
Data for wells and measured sections used in cross sections

Datapoint:	**Location:**		**Other:**		**Production:**		**Tops:**			
Name/UWI/API	SURFLAT	SURFLON	TD	SPUD_DATE	CUMOIL	CUMGAS	Top Neslen (MD)	Lower Farrer FS (MD)	Upper Farrer FS (MD)	Top Farrer Fm. (MD)
	Deg:Min:Sec	Deg:Min:Sec			BBLS	MCF	JA_NESL [ASC	JA_FARR_FS [	JA_FARR_FS2	JA_FAR [ASCH
4300710480	39:45:33.51	-110:47:08.5	3154.00	10/18/1956	0	104,800,000	1995.59	1528.37		1070.65
4300710752	39:42:10.05	-110:21:34.9	9644.00	08/29/1965	0.00	0.00	7398.59	7213.97		7013.23
4300710753	39:46:37.66	-110:27:59.7	12646.00	02/28/1981	1.00	0.00	5086.40	4840.81		4554.44
4300720253	39:44:27.75	-110:35:28.3	3520.00	08/02/1967	0.00	0.00	2304.37	2100.63		1784.52
4300720286	39:45:02.29	-110:15:34.3	17261.00	11/13/1967	0.00	202,860,000	6497.97	6305.18		6084.66
4300720352	39:46:30.10	-110:17:35.8	9802.00	10/27/1951	0.00	203,520,000	6388.66	5954.79		5694.11
4300730019	39:45:55.05	-110:16:17.4	7217.00	06/30/1974	2.00	0.00	7110.02	6882.26		6663.44
4301510800	39:19:11.20	-110:07:27.4	8480.00	07/03/1962	0.00	0.00	649.20	361.62	166.61	69.75
4301530080	39:24:48.91	-110:11:17.6	12706.00	10/07/1981	0.00	0.00	972.84	513.84		243.96
4301910084	39:09:58.14	-109:36:17.9	6801.00	06/11/1962	0.00	9.00	2094.83	2056.89	1675.66	1528.18
4301915047	39:25:30.48	-109:08:25.2	5725.00	05/29/1960	6.00	1.00	2911.03	2495.67	2230.47	1669.88
4301915662	39:20:48.68	-109:18:32.4	6550.00	12/13/1963	1.00	3.00	1683.02	1533.23	1071.29	986.82
4301915885	39:24:07.21	-109:08:37.8	6835.00	02/05/1956	9.00	4.00	1688.34	1592.89	1363.58	978.40
4301915889	39:24:11.90	-109:09:30.3	6575.00	08/26/1961	5.00	9.00	1551.14	1375.92	1203.77	739.77
4301930545	39:22:49.98	-109:16:28.9	7200.00	07/08/1980	6.00	4.00	2249.50	2227.50	1938.38	1746.34
4301930645	39:26:34.79	-109:09:50.0	7780.00	09/24/1980	9.00	0.00	2894.85	2654.69	2408.11	1703.96
4301930646	39:27:00.38	-109:09:01.3	7475.00	09/21/1980	4.00	0.00	2922.37	2525.19	2250.69	1506.97
4301930686	39:26:12.42	-109:06:32.8	6600.00	04/11/1981	6.00	0.00				
4301931253	39:25:04.44	-109:09:32.1	7053.00	01/12/1988	3.00	2.00	1748.00	1594.15	1338.26	1020.90
HorseCanyon(HCF-01)	39:28:18.62	-110:20:29.7	980.00				994.73	741.66		447.59
ThompsonCanyon(ThF-01)	39:00:00.37	-109:42:57.8	1000.00				879.79	819.23	426.31	18.51
GreenRiver(GRF-01)	39:11:48.84	-110:03:46.1	780.00				743.54	475.37	213.85	139.85
FloyCanyon(FLF-01)	39:01:31.55	-109:51:14.8	790.00				766.75	736.02	505.07	58.50
NineMileCanyon(NMF-01)	39:42:49.03	-110:36:24.8	550.00				515.97	271.27	206.56	2.03
CottonwoodCanyon(CCF-01)	39:10:33.69	-109:26:01.7	760.00				727.08	680.00	302.97	39.43
HaysCanyon(HAF-01)	39:16:58.89	-109:19:05.9	860.00				797.61	690.08	206.88	106.52
SanArroyoCanyon(SACF-01)	39:21:28.89	-109:11:25.7	905.00				897.68	819.77	650.29	296.48
WillowCreek(PRF-01)	39:46:04.01	-110:48:39.1	1100.00				1252.42	910.80		427.66
PriceCanyon(HK)**	39:43:54.55	-110:52:01.0	2100.00				1577.70	1307.89		901.01
TusherCanyon(HK)**	39:06:02.34	-110:01:17.9	2800.00				1281.94	987.14	753.05	385.33
GreenRiver(HK)**	39:11:41.32	-110:04:33.3	2350.00				1433.48	1015.63	798.21	675.11
HorseCanyon(HK)**	39:27:48.10	-110:20:48.1	1200.00				579.14	312.67		82.07

** "HK" indicates section source from Hettinger and Kirschbaum, 2002

Plate 1

Cross-section #1

Willow Creek to Floy Canyon, UT

Horizontal Scale = 5694.7
Vertical Scale = 25.0
Vertical Exaggeration = 227.8x

TOPS AND MARKERS

- JA_FAR ASCHOFF (Top Farrer Fm.)
- JA_ANCM ASCHOFF (Anchor Mine Flooding Surface)
- JA_NESL ASCHOFF (Top Neslen Fm.)
- JA_FARR_FS ASCHOFF (Lower Farrer Flooding Surface)
- JA_FARR_FS2 ASCHOFF (Upper Farrer Flooding Surface: less certain)

Plate 2
Cross-section #2
Floy Canyon, UT to UT-CO State Line
Horizontal Scale = 2079.6
Vertical Scale = 25.0
Vertical Exaggeration = 83.2x
TOPS AND MARKERS
JA_FAR ASCHOFF (Top Farrer Fm.)
JA_ANCM ASCHOFF (Anchor Mine Flooding Surface)
JA_NESL ASCHOFF (Top Neslen Fm.)
JA_FARR_FS ASCHOFF (Lower Farrer Flooding Surface)
JA_FARR_FS2 ASCHOFF (Upper Farrer Flooding Surface: less certain)
SEGO UOGC (Top Sego Sandstone from UOGC)
CASTLEGATE UOGC (Top Castlegate Sandstone from UOGC)
Rel Depth(ft)
<7.63MI>
<12.91MI>
<9.22MI>
<9.64MI>
<4.43MI>
<2.96MI>
<4.77MI>
<3.56MI>
<1.01MI>
<1.36MI>
<3.02MI>
<1.76MI>
<1.80MI>
JA_FAR [ASCHOFF]
JA_FARR_FS2 [ASCHOFF]
JA_FARR_FS [ASCHOFF]
JA_NESL [ASCHOFF]
SEGO [UOGC]
FloyCanyon(FLF-01)
ThompsonCanyon(TNF-01)
Outcrop GR curve right
NORTH CIS
4301910084
CottonwoodCanyon (CCF-01)
HaysCanyon (HAF-01)
WESTWATER
4301915662
FEDERAL 2
4301930545
SanArroyoCanyon (SACF-01)
SAN ARROY
4301915889
SAN ARROY
4301931253
SAN ARROY
4301915885
FED 6-4-1
4301930645
WESTBIT U
4301915047
FED 13-3-
4301930646